J. C. Schön, M. Jansen
Max-Planck-Institut für Festkörperforschung, Stuttgart, Germany

Prediction, determination and validation of phase diagrams via the global study of energy landscapes

Traditionally, the determination of phase diagrams has followed the inductive paradigm, where experimental observations provide the phase boundaries in more or less detail and phenomenological and semi-phenomenological models are employed to interpolate between the experimental data points, and by extrapolation to predict the shape of the phase boundaries in experimentally inaccessible regions. Over the past fifteen years, a new methodology has been developing, the aim of which is the prediction, determination and validation of phase diagrams in chemical systems without any recourse to experimental information. The founding stone of this deductive approach is the global study of the energy landscape of the chemical system. In this review, we present an introduction to the concept of energy landscapes in the context of phase diagram calculations, an overview over the large variety of methods employed to study energy landscapes and compute free energies on the ab initio level, and a number of typical examples of first-principle predictions, determinations and validations of phase diagrams.

Keywords: Phase diagram; Energy landscape; Structure prediction; Free energy computation; Phase diagram determination

1. Introduction

Among the fundamental areas of physics such as classical mechanics, electromagnetism or quantum mechanics, thermodynamics has always occupied a special place. It is not based on the behavior and treatment of idealized microscopic discrete entities such as individual particles or charges, or continuous fields, but has its origin in the macroscopic world predating the triumph of the atomic hypothesis by many decades [1, 2]. Yet at the same time the laws and concepts of thermodynamics show an enormous richness: they emerge from and at the same time transcend classical and statistical mechanics, are interwoven with all fields of physics, and reach beyond physics into all areas of natural science and are even found in fields like computer science [3, 4] or economics [5, 6], wherever statistical quantities and stochastic processes are encountered. One of the basic features of thermodynamics is the concept of a phase diagram [7–9], originally conceived in solid state chemistry and metallurgy as a tool to represent experimental facts about which phase of a material (classically: solid, liquid or gas) is present at what thermodynamic conditions, i.e. at what values of the thermodynamic state variables (classically: pressure (volume), temperature, and mole fractions). Nowadays, phase diagrams are found in many areas of science ranging from algorithmic theory [10] over the whole field of physics [11–13] to economics and even philosophy.[1] However, in this work, the focus will be on phase diagrams of chemical matter.

Considering its heritage in macroscopic physics and chemistry, the wide-ranging applicability and the great success of thermodynamics when dealing with macroscopic entities, it is no surprise that in many fields of science thermodynamics and thus also phase diagrams have become established as independent topics of research that are only weakly linked in the mind of the practical, usually experimental, materials scientist and engineer to the underlying behavior of the atomic constituents of matter.[2] Since thermodynamics is in many ways a mathematically self-contained subject, dealing with the thermodynamic properties of macroscopic matter without any input from the atomic level has been extraordinarily successful. One notes that neither Gibbs' phase rule nor a rudimentary phenomenological theory of phase transitions on the level of the Clausius–Clapeyron equation require input from outside fields such as statistical mechanics.[3]

However, this self-sufficiency reaches its limits once we are interested in thermodynamic conditions where experimental data are no longer available or become highly unreliable, or if we try to envision hypothetical not-yet synthesized compounds [23–25] and attempt to derive the phase diagrams where these compounds might appear. Trying to address issues like these has led to the introduction of many concepts, methods and models from statistical mechanics into thermodynamics in general [16, 17] and the study of

---

[1] In the philosophy of Hegel [14] and his successors, the image of a phase change from water to vapor is used to illustrate the transformation from quantitative to qualitative change, e.g. in society.

[2] And there is some truth to this gut-feeling; one need only recall the still debated issue of how ergodicity and irreversibility emerge from the dynamics (classical or quantum) of the multitude of particles macroscopic entities are composed of [15].

[3] Even simple nucleation theory can be largely formulated within a macroscopic thermodynamic framework [16–22].

phase diagrams in particular [7, 26].[4] For most purposes, the fundamental link between the two fields are the state functions such as the Helmholtz free energy $F(N_i, V, T)$, the Gibbs free energy or free enthalpy $G(N_i, p, T)$, etc., which on the one hand can be computed on the basis of equilibrium statistical mechanics and on the other hand serve as the starting point for many calculations in thermodynamics [28]. In the context of phase diagrams, two important questions are being addressed: 1) Given a chemical system in a known particular state, what is the corresponding Gibbs free energy (sometimes also called the characteristic function, the isothermal-isobaric thermodynamic potential, the free enthalpy, or just the Gibbs energy), and how does this value compare with the Gibbs free energy of known alternative phases of the system that are compatible with the external thermodynamical conditions? 2) More fundamental is the second question: what possible stable phases or combinations thereof can the system exhibit for given values of pressure, temperature etc., and what is the role played by the so-called metastable phases that are not included in the conventional presentation of phase diagrams?[5] In particular, the prediction of new thermodynamically stable solid phases at low and intermediate temperatures and similarly at high pressures is of great interest since the search for new modifications in these regions of the phase diagram via experiments is often severely impeded because synthetic and/or analytical methods are lacking to properly explore the full range of possible stable and metastable phases.

Historically, the first question has taken precedence, starting with the introduction of phenomenological models [9] for phases such as the ideal and regular solution models, lattice based approaches such as sublattice models, the compound energy formalism [29], and associated solution models [30], until we are now exploring various classes of cluster expansion and cluster variation models [31]. One focus in these approaches has been to interpolate between experimentally determined datapoints along phase boundaries when constructing phase diagrams, and this research has culminated in the on-going CALPHAD project [9, 32–36] and the development of a number of automated programs [37–40] that allow the computation of phase diagrams by combining experimentally determined Gibbs free energies with flexible model descriptions containing a number of fit parameters. Parallel to the CALPHAD effort, much work has been performed in trying to provide theoretically computed free energies for those regions of the phase diagram where the thermodynamically stable phases are known but the free energies are difficult to determine experimentally. Here, much progress has been made since the early 1990s [41–48] when the large increase in computer power has put into our reach both quantum mechanical computations of ground state energies, defect energies and vibrational densities of states, and classical molecular dynamics and Monte Carlo simulations of free energy differences using highly refined empirical potentials.

But the early 1990s have also seen the beginning of the development of methods to address the second fundamental issue mentioned above, i. e. which hypothetical modifications can exist for given pressure and temperature, where the focus has been on the low temperature and high pressure regions of the phase diagram [49–52]. As we will discuss in the following section, the foundation of all these methods is the energy landscape [23–25, 53–56] of the chemical system under consideration. A complete knowledge of this landscape allows us, in principle, to determine not only the existence of kinetically and thermodynamically stable phases, but also the degree of their stability and their atomic transformation routes during phase transitions.

In this review, we will present the general outline of the energy landscape approach to the prediction of phase diagrams, followed by a short overview over the most important methods currently employed to identify new phases and to compute their free energies. This more technical section is followed by the presentation of a number of examples of the ab initio computation of phase diagrams or parts thereof, with no information from experiment, and some examples describing the current state of the field as far as the computation of phase diagrams is concerned once the possible or expected phases are known.

Due to the space limitations of this review, we cannot touch upon equally fascinating aspects such as the 'phase diagrams' of finite size systems such as clusters [57–59], the thermodynamics of structurally disordered systems such as glasses [60], phase diagrams and phase transitions due to magnetic, elastic, or electric interactions [13], quantum phase diagrams [12], or phase diagrams in complex systems not based on materials [10]. All these systems can also be studied within the context of an energy or cost function landscape over a continuous or discrete configuration space, of course. For more details, we have to refer the interested reader to the literature on these systems.

2. First principles approach to the computation and prediction of phase diagrams

Starting point for any prediction of phase diagrams without recourse to experimental information is the representation of the chemical system at hand as a collection of N atoms. Classically, this translates into describing the system at each moment in time by two $3N$-dimensional vectors, $\vec{R} = (\vec{r}_1, \ldots, \vec{r}_N)$ and $\vec{P} = (\vec{p}_1, \ldots, \vec{p}_N) = (m_1\vec{v}_1, \ldots, m_N\vec{v}_N)$, giving the positions and momenta of all atoms as a function of time. The energy of this system is given by the sum of the kinetic and potential energies, $E_{\mathrm{kin}} = (1/2)\sum_i m_i(\vec{v}_i)^2$ and $E_{\mathrm{pot}} = E_{\mathrm{pot}}(\vec{r}_1, \ldots, \vec{r}_N)$, and the dynamics follows from Newton's equations, with the forces computed by taking the gradient of the potential energy. As long as we can invoke the Born–Oppenheimer approximation and neglect zero point vibrations – the usual case –, this picture also applies in a quantum mechanical treatment after integrating out the electronic degrees of freedom. Since the dependence of the kinetic energy on the momenta is just a quadratic function and the potential energy (in non-magnetic systems) only depends on the positions of the atoms, the

---

[4] Of course, the question to what extent thermodynamics can be actually derived from statistical mechanics and ultimately from classical and quantum mechanics, has been another crucial motivation for studying the connection between thermodynamics and statistical mechanics [15, 27]. In this review, we are not discussing this more fundamental issue but focus on the more practical application of statistical mechanics to phase diagrams.

[5] One should recall that a large number of the materials used in everyday life are actually not thermodynamically stable but only metastable. Nevertheless, they are of great practical importance because they are kinetically stable on the typical time scales of interest.

dynamics of the system are given once the hypersurface of the potential energy over the $3N$-dimensional space of all atom arrangements, the so-called configuration space of the system, is known. This energy hypersurface is commonly denoted as the energy landscape of the chemical system [23–25, 53–56].[6]

The crucial step in going from the classical mechanical description above to the thermodynamic one is the determination of the so-called locally ergodic regions on the energy landscape [55]. For a given temperature T, a subset $\mathcal{R}$ of the configuration space is called locally ergodic on the observation time scale t_{obs}, if the time $\tau_{\mathrm{eq}}(\mathcal{R};T)$ it takes for the system to equilibrate within $\mathcal{R}$ is much shorter than t_{obs}, while the time $\tau_{\mathrm{esc}}(\mathcal{R};T)$ it takes for the system to leave the region $\mathcal{R}$, the so-called escape time, is much larger than t_{obs},

$$\tau_{\mathrm{esc}}(\mathcal{R};T) \gg t_{\mathrm{obs}} \gg \tau_{\mathrm{eq}}(\mathcal{R};T) \tag{1}$$

If this holds true, then the ergodic theorem tells us that we can replace the time averages of observables $O(\vec{R}(t), \vec{P}(t))$ along a trajectory of length $t_{\mathrm{obs}} = t_2 - t_1$

$$\langle O \rangle_{t_{\mathrm{obs}}} = \frac{1}{t_{\mathrm{obs}}} \int_{t_1}^{t_2} O(\vec{R}(t'), \vec{P}(t'))\, \mathrm{d}t' \tag{2}$$

inside the locally ergodic region $\mathcal{R}$ by the (Boltzmann) ensemble average of this observable

$$\langle O \rangle_{\mathrm{ens}}(T) = \frac{\int O(\vec{P},\vec{R}) \exp(-E(\vec{P},\vec{R})/k_{\mathrm{B}}T)\, \mathrm{d}\vec{P}\, \mathrm{d}\vec{R}}{\int \exp(-E(\vec{P},\vec{R})/k_{\mathrm{B}}T)\, \mathrm{d}\vec{P}\, \mathrm{d}\vec{R}} \tag{3}$$

restricted to the region $\mathcal{R}$,

$$|\langle O \rangle_{t_{\mathrm{obs}}} - \langle O \rangle_{\mathrm{ens}}(T)| < a \tag{4}$$

Of course, this 'equality' holds only within an accuracy a, since only local and not global ergodicity is assserted.[7] In particular, we can compute for every locally ergodic region $\mathcal{R}_i$ the local free energy

$$\begin{aligned} F(\mathcal{R}_i, T) &= -k_{\mathrm{B}} T \ln Z(\mathcal{R}_i, T) \\ &= -k_{\mathrm{B}} T \ln \sum_{j \in \mathcal{R}_i} \exp(-E(j)/k_{\mathrm{B}}T) \end{aligned} \tag{5}$$

and thus apply the usual laws of thermodynamics to the system as long as it remains within the region $\mathcal{R}_i$. Figure 1 depicts a sketch of a simple two-dimensional landscape where the locally ergodic regions are indicated.

For any given observation time scale t_{obs}, the configuration space of the chemical system is split into a large number of disjoint locally ergodic regions, with the remainder of the configuration space consisting of transition regions connecting the locally ergodic regions. Each such region corresponds to a kinetically stable compound of the chemical system on the time scale of observation. It is important to note that the set of all locally ergodic regions on an energy landscape depends not only on the observation time chosen, but also on temperature since the escape time in particular tends to vary strongly with temperature. As long as the probability of being found in one of these locally ergodic regions is much larger than the probability of being found in a transition region,

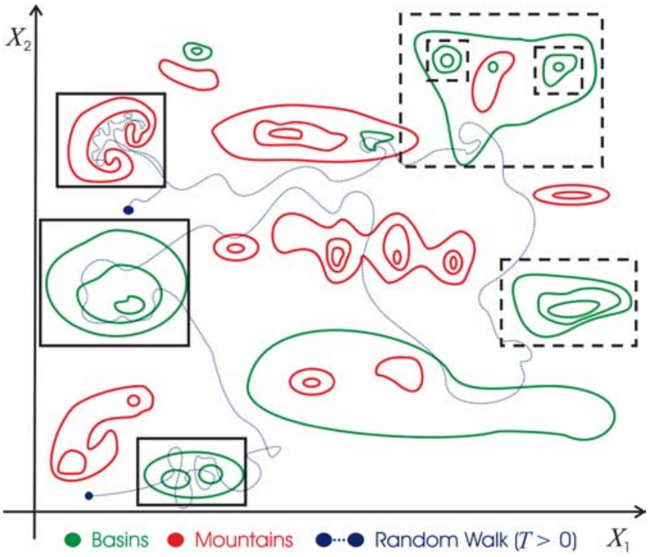

Fig. 1. Sketch of an energy landscape consisting of minima regions (green level lines) and mountain regions (red level lines). Blue dotted line indicates trajectory of the system. Regions contained in black rectangles are locally ergodic regions on the time scale of observation encountered during the simulation; dashed black rectangles are locally ergodic regions that have not been visited during this particular simulation run. Note that locally ergodic regions do not have to contain a local minimum – entropic barriers can be sufficient to establish local ergodicity [61].

$$\frac{\sum_i p(\mathcal{R}_i)}{1 - \sum_i p(\mathcal{R}_i)} \gg 1 \tag{6}$$

where

$$p(\mathcal{R}_i) = \sum_{j \in \mathcal{R}_i} p(j) = \sum_{j \in \mathcal{R}_i} \frac{\exp(-E(j)/k_{\mathrm{B}}T)}{Z} \tag{7}$$

the system can be considered to be in (meta)stable thermodynamic equilibrium on the timescale t_{obs}.[8] Note that if the system has been given an essentially infinite time $\tau_{\mathrm{eq}}^{\mathrm{global}} \gg \tau_{\mathrm{esc}}(\mathcal{R}_i)$ to equilibrate before we perform our measurement on the timescale t_{obs}, the system can be treated as globally ergodic, and the likelihood of finding the system at the time of the measurement in a particular locally ergodic region $\mathcal{R}_i$ is given by $p(\mathcal{R}_i)$. As a consequence, the locally ergodic region with the lowest free energy has the highest probability of being occupied during the measurement, and the compound corresponding to this region is customarily designated to be the thermodynamically stable phase.[9]

---

[6] In a full quantum mechanical description, we also need to take additional electronic and spin degrees of freedom into account. For clarity of the presentation, we only discuss in this section the classical system without electric and magnetic fields.

[7] For a more detailed discussion of local ergodicity, see e.g. Refs. [55, 61]. Other concepts closely related to locally ergodic regions are the so-called 'stable states', 'subcanonical ensembles' and 'wells', respectively [27, 62–65].

[8] This condition does not hold e.g. if the system has a high tendency to form glassy phases.

[9] We have to be careful not to run into a seeming paradox here: the system is globally equilibrated on the time scale $\tau_{\mathrm{eq}}^{\mathrm{global}}$, where all the regions that are locally ergodic on the time scale t_{obs} have interacted since $\tau_{\mathrm{eq}}^{\mathrm{global}}$ is much larger than the escape times from the

Quite generally, one notes that at low temperatures, the escape times from the locally ergodic regions tend to follow an Arrhenius law and are therefore controlled by energetic barriers on the energy landscape. Thus, at very low temperatures individual local minima[10] of the energy landscape are locally ergodic and their local free energies are determined by the energy of the minimum plus the contribution of the vibrations about these minima[11]. Usually, the regions with the lowest free energy correspond to crystalline modifications of the system, while structures containing defects are also associated with local minima but with higher energies.[12] At elevated temperatures and on sufficiently long time scales, locally ergodic regions will typically encompass many local minima. The most common case is that the region consists of a large basin containing both the perfect crystalline minimum and the minima corresponding to equilibrium defects of this structure.[13] Other very important examples are locally ergodic regions that contain all the local minima associated with, for example, the rotation of complex anions in a solid or the oscillation of individual atoms in double-well potentials, or the many local minima representing possible atom arrangements belonging to solid solutions or alloy phases. At even higher temperatures, essentially all locally ergodic regions merge on the observational time scale, melting occurs, and the system is no longer found in the solid but in the liquid state.

Constructing an equilibrium phase diagram from first principles thus involves as a first step the determination of the locally ergodic regions on the energy landscape of a chemical system as a function of temperature, pressure and concentration of the different types of atoms for observational time scales of interest. Next, the local free energies of the corresponding (metastable) compounds and phases are computed and by minimization of these free energies the thermodynamically stable phase is obtained. While this general approach is very straightforward in principle, there are a number of issues and practical limitations that need to be addressed when designing an efficient implementation.

In principle, the determination of locally ergodic regions consists of three steps: the generation of a candidate for such a region, the verification that the candidate is locally equilibrated on the time scale of observation, and the verification that the candidate is kinetically stable on the time scale of observation [66]. Three main classes of approaches to generating structure candidates exist in the literature: direct determination of local minima and structure families of such minima on the energy landscape [23–25, 66], chemically inspired [67–71] and/or systematic construction [72, 73] of hypothetical candidates including database-driven searches [74, 75] and topological bond-network methods [76–82], and dynamical simulations that try to reproduce or imitate chemical and physical processes such as pressure or temperature induced solid–solid phase transitions [83–86], the sol-gel process [87, 88], or crystallization from solution [89] or the melt [90]. One should note that the next steps of verifying that these candidates are equilibrated and kinetically stable are in most instances reduced to only checking whether the candidate corresponds to a local minimum of the energy. The reason for this is that further investigations such as the determination of the energetic and entropic barriers surrounding the locally ergodic regions are still far from trivial and require a very large computational effort, especially if one attempts to compute these barriers on the ab initio quantum mechanical level. Such computational limitations are also the reason why the systematic determination of all relevant local minima on an energy landscape without any direct or indirect input from experiment is still at the border of our abilities for systems with more than about 40 atoms/simulation cell, irrespective of the global search algorithm employed. In contrast, there is no in-principle problem in constructing candidates by copying and modifying known structures of chemically (more-or-less) related compounds from various databases or in generating periodic bond-networks for a given set of allowed bond-connectivities. The main problem of the database driven approaches is the fact that during global optimizations on energy landscapes one often finds energetically very low-lying minimum structures that do not exist in databases or do not obey the topological rules. Regarding the topological network approach, one could in principle construct all possible atom-networks by including many different types of bond-connectivities into the topological network generation, but then the number of hypothetical candidates would grow exponentially fast with the number of atoms/cell [76], and the local minimizations required for these network-based structure candidates would also overwhelm the computational resources.[14] The issue of computational resources obviously also confronts the third class of approaches, of course.

Regarding the computation of free energies of the candidates for locally ergodic regions, a number of established methods exist: direct calculations by, for example, adding

---

individual locally ergodic regions, $\tau_{eq}^{global} \gg \tau_{esc}(\mathcal{R}_i)$. Probabilistic arguments then suggest that we will most likely encounter the system in the phase with the lowest free energy. (In the thermodynamic limit, this probability becomes overwhelmingly large.) However, our actual measurement takes place on a much shorter time scale $t_{obs} \ll (\mathcal{R}_i)$ (but $t_{obs} \ll \tau_{eq}(\mathcal{R}_i)$), on which the individual regions $\mathcal{R}_i$ are locally equilibrated but are effectively decoupled from the remainder of the energy landscape. An example might be the measurement of the powder diffractogram of a phase separated solid solution that only requires a couple of hours measurement time, after the system has spent several months relaxing from an originally homogeneous metastable quenched solid solution phase in to the thermodynamically stable two-phase state.

[10] Both the perfect crystalline atom arrangement and defect configurations constitute such individual local minima.

[11] Recall that magnetic and electronic degrees of freedom are excluded in this discussion.

[12] Of course, on long enough time scales $t_{obs} \gg \tau_{eq}^{defects} \gg \tau_{esc}(\mathcal{R}_{cryst}), \tau_{esc}(\mathcal{R}_{def})$, the system can establish local equilibrium between the minimum corresponding to a perfect crystalline atom arrangement R_{cryst} and the defect minima $\mathcal{R}_{def}$ even at very low temperatures. In such a case, the locally ergodic region encompasses a larger basin around the crystalline minimum containing many side minima, and the free energy includes a contribution due to the various equilibrium defects. Nevertheless, if the actual measurement were to be performed on much shorter time scales $t_{obs} \ll \tau_{esc}(\mathcal{R}_{cryst}), \tau_{esc}(\mathcal{R}_{def}) \ll \tau_{eq}^{defects}$, the defect contribution to the free energy would not be observed.

[13] Non-equilibrium defects cannot be part of a locally ergodic region, by definition. In practice, we can actually classify the regions that are locally ergodic on the time scale t_{obs} by the type and number of kinetically stable non-equilibrium defects (e. g. the set of pinned grain boundaries in a crystal).

[14] In the extreme case, we would essentially scan the configuration space more or less densely, a method often employed when predicting possible structures of molecular crystals using (rigid) unbreakable molecules [72].

the phonon contribution of the free energy to the minimum energy of the structure, and indirect computations by evaluating the free energy difference between the candidate and another system with known free energy, or by analyzing the phase space volume seen during long dynamical simulations. Regarding the last two methodologies, the computational requirements again are critical insofar as one needs both sufficient statistics and a reasonably high accuracy of the energy calculations that should be either on the ab initio level or using a refined empirical potential, in order to reach good quantitative agreement with experiment.

3. Methods

Three classes of computational tools have to be provided in order to predict and validate phase diagrams: tools to explore energy landscapes, tools to compute free energies, and tools to compute phase diagrams. We will not touch on the last one, since a number of program libraries are available for this purpose [37–40, 91] with most of them having grown out of the CALPHAD project [9], and focus instead on the other two in this review.

3.1. Tools to explore energy landscapes

Central quantities of interest of energy landscapes are special points [92] such as local minima and saddle points (in particular those connecting pairs of minima), special regions such as locally ergodic regions [55], transition regions [93] and normal hyperbolic manifolds [94, 95], local densities of states, and the flow of probability on the landscape with the corresponding barrier landscape consisting of (generalized) barriers [61] such as energetic, entropic and kinetic barriers [96]. Finally, visualization plays an important role, in order to represent the high-dimensional complex multi-minima landscape in a simplified fashion; here, graph-based representations [97] and the reduction of the number of relevant coordinates [98] are the most important tools.

3.1.1. Identification of local minima

A large number of methods to identify local minima on the energy landscape have been developed for the solution of discrete and continuous optimization problems in mathematics, physics, chemistry, biology etc., and have been adapted and applied to the issue of identifying structure candidates in chemical systems. The two crucial issues are the efficiency of the search, and the effect of simplifications and modifications of the energy landscape with the goal of speeding up the search procedure. One should note that we are not only interested in the global minimum – all minima with low energies and sufficiently high barriers surrounding them are of importance since they represent potentially valuable metastable compounds.

The most simple approach is the use of multiple quenches, i. e. for a given starting point, neighbor configurations with lower energy are found deterministically (e. g. via computation of the gradient) or stochastically, and this downhill search continues until the system has reached a local minimum. This procedure is repeated for a very large number of starting points that are generated either by systematically or randomly scanning the configuration space [99] or by chemically inspired choices [69], e. g. via network model generation [100–102] or selection of structures from databases [74, 103]. A similarly straightforward approach consists in performing long Monte Carlo or molecular dynamics (MC/MD) simulations at constant temperature, where periodically quenches are performed along the trajectory of the system [104, 105]. Here, one often speaks of a ‘walker’ and his trajectory on the landscape.

Related to this approach is the so-called simulated annealing [106, 107], where during the MC/MD simulations the temperature is decreased, in order to focus the exploration on regions where deep-lying minima are expected to be found. If one performs an MC simulation, one can replace the physically realistic moveclass of moving one or a few atoms by a small amount by a more optimization effective moveclass that allows larger changes in the atom configuration during each move, in order to explore a larger part of the landscape. In this case, it is sometimes efficient to combine such large moves every time with a quench; this scheme is often called basin hopping [108, 109]. Besides the moveclass, there are a number of other features of simulated annealing that can be adjusted to increase the efficiency of the algorithm [4, 110]. The temperature schedule $T(n)$, where n counts the number of moves along the trajectory, can be optimized; common schedules are exponential or linear decrease with n, schedules involving temperature cycling [111, 112] where the temperature periodically increases and then decreases again, and adaptive schedules [3, 113] that take properties of the landscape explored up to now into account. Multi-walker implementations have also been used [110, 114], such as the Demon-algorithm [115], methods that generate an averaged landscape [116–119] such as conformation-family Monte Carlo [120], superposition state molecular dynamics [121] and SWARM molecular dynamics [122], or multi-overlap dynamics [123–125], parallel tempering [126] and J-walking [127] where different walkers run at different temperatures and periodically switch positions (or temperatures), in order to overcome barriers more efficiently. Finally, the acceptance criterion can be modified; the most popular ones accept a move according to the classical Metropolis distribution [128], the Tsallis distribution [129, 130], or based on a temperature dependent acceptance-threshold [131].

A different class are the taboo searches [132–134], where one performs MC/MD simulations and already visited regions are forbidden, either by rigid exclusion constraints or via penalty terms added to the energy function [135]. A crucial issue here is the length of the memory chain; combining a taboo search with quenches and large moves as in basin hopping schemes can alleviate the memory problem to a certain extent [136]. One of the more recent incarnations of a taboo search is the metadynamics approach [137]. Furthermore, there exist a number of methods designed to achieve a more efficient barrier crossing, which are based on the modification and/or simplification of the energy landscape [135, 138–146], e. g. by locally elevating visited areas [135], by lowering barriers relative to the local minima [142], stochastic tunneling [143, 147–149], dynamic-lattice searching [150], or by modifying the potential between the atoms [140]. Typically, the landscape modifications during such accelerated (molecular) dynamics runs are adaptive, i. e., they vary with the progress of the simulation and depend on the information already gained about the system, in this way being related to the taboo-searches.

Genetic or evolutionary algorithms have become very popular over the past decade [151–158]. They are essentially a deterministic or stochastic evolution of an interacting ensemble of walkers which exchange information not only about the regions of the landscape explored but also by generating new configurations via a mixture (cross-over move) of two or more walkers, in addition to simple modifications of individual walkers (mutation move). A feature of great importance is the representation of the members of the ensemble for the purpose of cross-over moves, i. e. either as a genotype [159] (discrete encoding of an atom configuration) or as a phenotype [152, 160, 161] (the actual atom configuration) where in the latter case one often adds a local minimization after the cross-over has taken place [152, 162].[15] One problem with evolutionary algorithms is the limited physical realism of the moveclass which makes it difficult to estimate the stability of the minima and can lead to the elimination of a number of local minima. Here, one should also mention extremal optimization [149, 163], which is an ensemble-based exploration approach that produces a very wide spread in the energy distribution of the local minima that can be potentially quite useful when dealing with large energy barriers on the landscape.

Exhaustive searches are most common if the energy landscape is discrete or can be easily discretized via fast local minimizations. Branch-and-bound methods [164, 165] can be quite effective and similarly the lid algorithm [166–168] which is based on a complete enumeration of all states reachable from a starting point without crossing a sequence of prescribed energy lids.[16] Again, the moveclass one uses for optimization purposes is often not necessarily a physically realistic one, and the system size can become a serious problem as the number of atoms/cell increases.

Finally, there exist several lid-based methods for continuous energy landscapes. Examples are the deluge algorithm [171], where an energy lid that must not be crossed during the random walk (like a Monte Carlo simulation where every move is accepted, i. e. where $T = \infty$) is slowly lowered from very high lid values, and the threshold algorithm [172] (originally developed as an implementation of the lid algorithm for continuous landscapes), where for a sequence of energy lids the walker is allowed to move below the lid, and one checks periodically whether new local minima have been reached by performing several quench runs from stopping points along the trajectories.

3.1.2. Identification of saddle points

Quite generally, the methods to find saddle points are considerably more involved and often less robust than the methods employed to determine local minima. One popular approach to identify saddle points proceeds by first finding the minima of the $|\nabla E|^2 (\geq 0)$ surface and then checking which among these points are actual saddle points of the original energy surface [173].[17] An alternative method is the slowest slides procedure and closely related methods [57, 174–176], where one follows along the slowest downhill eigenvector direction at any given point on the energy hypersurface until only one negative eigenvalue remains. Next, one follows this direction up to the saddle, and then from the saddle one can reach the minima (or perhaps further saddles) that are connected by the saddle at hand. This method is also slightly related to the conjugate peak refinement approach [177]. Complications can arise in particular when the steps of sliding and following the negative curvature need to be mixed.

Another class of procedures starts from one or more local minima and attempts to identify the nearest or lowest saddle to or between the minima, respectively. Eigenvector following [178, 179] proceeds in the direction of the softest eigenvector uphill out of the local minimum until a negative curvature appears; then one follows this direction uphill to the saddle. A contentious issue is whether one reaches really the lowest accessible saddle points. If two minima in close proximity are known, one can use elastic band methods [180–182] to first define the shortest path in configuration space between the two minima and then perform a local minimization along this path while not allowing the path to rupture. The maximum along the path generated via these minimizations is the saddle point. Choosing the appropriate path is a major issue here, in particular if the two minima are not nearest neighbors but are separated by several saddle points. One should note that such activation–relaxation techniques [183–185] that identify saddle regions can also be employed to detect neighboring minima.

3.1.3. Identification of locally ergodic regions

The most straightforward approach applicable for low temperatures consists in finding the local minima of the energy landscape as discussed above and checking that they are surrounded by sufficiently high energy barriers [172, 186]. At higher temperatures, one can use long Monte Carlo or molecular dynamics simulations and attempt to visually identify stable structures about which the system oscillates, even if the structure does not correspond to a single, or even any, local minimum of the energy landscape [83, 86, 187]. A more systematic approach is the so-called ergodicity search algorithm [188], where one registers the fluctuation of indicator variables, for instance the potential energy or the radial distribution function, within time windows during the long simulations. If the average value of these variables jumps between two windows by more than the fluctuation, this suggests the existence of a new locally ergodic region. Next, swarms of short simulations starting from points along the trajectory in the time window are employed to verify whether the system is in local equilibrium in this region, and long simulations for a number of temperatures are used to measure the probability flow from the region and thus the escape time. Unsurprisingly, searching for locally ergodic regions in this fashion is quite expensive computationally.

3.1.4. Analysis of transition paths

The search for the transition path between two locally ergodic regions representing two phases [189, 190] is an impor-

---

[15] Quite generally, methods where stochastic moves are combined with local minimizations are often denoted as hybrid methods.

[16] As happens a lot in this field, this algorithm has also been re-invented [169, 170].

[17] Note that not every point which fulfills the requirement $\nabla|\nabla E|^2 = \vec{0}$ is a critical point of the energy hypersurface.

tant task when studying the stability of phases, the transitions among them, and the mechanism of chemical reactions. Much work has been performed by postulating a reaction coordinate and approximately following this route [191, 192]. The first class of methods that attempt to find such paths without prior chemical information or inspiration are the so-called elastic band methods mentioned above, which are most efficient at low temperatures and if the minima are reasonably close together. However, both the individual phases and the transition regions tend to contain many minima, in particular defect structures within the locally ergodic regions and complex pre-nucleation structures inside the transition regions, which can make the choice of a 'shortest path' between the two phases quite unrealistic. Alternative methods are in particular the so-called transition path sampling [64, 193–195], where one performs essentially a Monte Carlo walk on the space of transition paths, and related procedures [182, 196–199]. One attempts to match forward and backward routes between the two minima along molecular dynamics simulations of a single path. The sampling of path space takes place via small changes in the initial conditions of the forward and backward path simulations. Finally, one can compute the reaction rates via transition state theory [200–203].

The metadynamics scheme [137] mentioned and related methods [204, 205] provide an alternative, where only a starting minimum/phase is provided, and one expects the system to find the new phase 'on its own', by slowly building up a penalty type potential inside the starting region which makes the starting region energetically unfavorable and forces the walker to leave the region. This taboo-like search works in principle at any temperature, and one can measure the local free energy in the process, too [206, 207]. By performing quenches along the trajectory, one can find neighboring minima, analogously to e. g. the threshold algorithm [172, 208]. Just as the ergodicity search algorithm [188] relies on a sensible choice of indicator variables to identify candidates for new locally ergodic regions, the metadynamics requires a good choice of an order parameter, which allows distinguishing between the original phase and the new one(s), which is often a non-trivial issue. The same holds true for alternative methods such as some type of coarse molecular dynamics [209–214] or various steered dynamics procedures [215–221]. One should note that just as in the case of the saddle point determination, transition path sampling and metadynamics can be quite expensive computationally.

3.1.5. Measurement of probability flow

An issue closely related to the analysis of transition paths and the stability of locally ergodic regions is the measurement of probability flows among locally ergodic regions. If the transition paths are known and reasonably simple, one can employ standard transition state theory to compute the likelihood of moving between the various minima from the knowledge of the minima and the energy and width of the saddles. Similarly, if one particular transition is the focus of the study, transition path sampling will yield sufficient information to compute the probability flow.

More generally, one can employ many long standard constant temperature MC/MD simulations plus quenches, in order to measure the probability flow as a function of temperature. A major problem here is the required length of the simulations at realistic temperatures for reasonably sized systems. An alternative is the threshold algorithm mentioned above, where the probability flow is measured not as a function of temperature but instead as a function of energy slice for each energy lid [172, 186]. Similar to the metadynamics, no target is given, the density of states is sampled, and all minima that have been identified serve as starting points for threshold runs. By performing many quenches along the way, one can gain estimates on the energetic and entropic barriers and determine the size of the transition regions by identifying the so-called characteristic regions [93] as a function of energy slice. These characteristic regions are defined via the probability of reaching a set of minima from a given stopping point along a trajectory when one performs many stochastic quenches from the same stopping point.

3.1.6. Measurement of local and global densities of state

The most straightforward method to measure local densities of states is to sample them via long unbiased random walks [222, 223], and then to normalize them to, e. g., the vibrational density of states around local minima. The classical histogram methods belong to this group [224, 225]. The most obvious problem is the long simulation time; other issues are to separate the contributions of many different minima. As a consequence, re-weighting methods have been developed [226, 227], where one performs the simulations, for example, for many different temperatures and rescales the sampled densities of states with the acceptance probabilities such that the simulation effectively corresponds to diffusion on a 'flat' landscape. Many different schemes have been proposed to achieve this end: weighting of histograms on the fly, e. g. WHAM [228, 229], re-analysis of data of constant temperature runs taken e. g. from expanded ensembles [230], parallel tempering or multi-canonical simulations [125, 226, 231–238], modification of the landscape such that it effectively becomes flat while keeping track of the measured density of states [239] as in metadynamics simulations, global or local transformation of the landscape using e. g. hyperbolic functions to make the landscape look 'flat' and re-weight the sampled DOS afterwards [226]. Important issues are the statistics, of course, the homogeneous sampling of different metabasins containing many local minima, and the overlap of distributions taken at different temperatures.

Similar concerns arise when mapping the DOS measured within overlapping energy slices, with subsequent slice-matching as one does when using, e. g., the threshold algorithm [172]. The normalization in particular is usually performed with respect to the phonon spectrum of individual minima. For low temperatures, where most of the sampled DOS during a realistic physical trajectory inside a locally ergodic region comes from within the harmonic regions around the local minima and saddle points, one can use analytical methods to compute the density of states from the phonon spectrum of the Hessian of the minimum under consideration. Even anharmonic corrections [240, 241] and magnetic contributions [242–244] can be included to some degree. Alternatively, one can compute the phonon spectrum from simulations e. g. via the Fourier transform of the velocity autocorrelation function [245].

3.1.7. Landscape representations

Graph representations of energy landscapes are among the most popular ways to provide a simplified description of an energy landscape. In particular various types of tree graphs [97, 166, 172, 246–250] have been invented and re-invented many times. Here, the leaves of the tree represent local minima together with their basins up to the lowest saddle points where two such minima are connected. This connection is represented as another lumped node at the energy of the lowest connecting saddle point, and one continues this procedure until all minima are connected. Further developments in this direction are network-representations of landscapes [165, 251–259]. Similarly, a representation of the barrier structure and probability flows via transition probability matrices [166, 246, 260, 261] or transition maps [186], as a function of energy slice and/or as a function of temperature is quite common now. The same holds true for projections of the landscape onto reduced sets of coordinates [262] such as order parameters [16], essential subspaces [263] or so-called principal components [98, 264–266] which are equal to linear combinations of coordinates that are most meaningful to describe the static, dynamic and/or statistical properties of the atom configurations. Due to space constraints, we will not discuss landscape representations in more detail and refer the reader to the literature.

3.2. Tools to compute free energies

With regard to the computation of free energies, two different types of calculations need to be distinguished: energy landscape based methods, and procedures where the phase of interest encompasses so many local minima on the energy landscape that special tools based on statistical mechanical models are necessary to evaluate the free energy [45].

The most straightforward approach to computing the free energy of a system is via the (local) density of states of a region on the energy landscape that has been found using one of the methods described above. As far as the accuracy of such a procedure is concerned, the main issue is the quality of the density of states used as input for the calculation. A somewhat more subtle issue is the question to what extent, for example, methods that employ an order parameter for assigning the density of states to one or other of several minima actually produce the correct densities of states of locally ergodic regions, for which only the concept of a local free energy is cleanly defined. In the literature, one often finds plots of ‘free energies’ as a function of an order parameter, with ‘free energy barriers’ as a function of an order parameter between the two competing phases. As we indicated earlier, as long as one assumes that the system has had a sufficiently long time to equilibrate between the two phases, and the value of the ‘free energy’ as a function of an order parameter only signifies the probability that at any given moment one will encounter the system in a state that exhibits this order parameter value, there is no problem. But making dynamical statements about the transition region, e. g. by treating the set of configurations where the ‘free energy’ has a maximum as a function of the order parameter as a transition state with an associated free energy barrier, is highly problematic.[18]

One procedure that has been employed for many years is the computation of the free energy of a system A via the difference between two free energies belonging to systems A and B, where the free energy of system B usually serves as a reference energy that can be computed analytically (e. g. the free energy of a system of Einstein oscillators) or is known from very detailed computer simulations.[19] Three slightly different approaches have been developed for this purpose, called thermodynamic integration [268], thermodynamic perturbation [269] and computational alchemy [270]. One feature common to all of them is that we need to choose some path between the two systems, along which one smoothly transforms one of the two systems into the other, or moves phase A to phase B. The first two procedures employ umbrella sampling [271] via the overlap of probability distributions along the path, while the third one computes the total work employed when moving from system A to system B and back and uses these two values to determine bounds on the free energy difference between A and B. While the choice of path and the allocation of time along the path is very important for the efficiency of the algorithm [272], the path as such does not necessarily have to be dynamically meaningful. Nevertheless, sampling error inaccuracies are bedeviling essentially all numerical estimates of free energies derived from dynamical simulations [273].

When studying two different phases, one can also compute the free energy along a chosen path, e. g. in order parameter space or along a reaction coordinate via integration over the remaining coordinates [274, 275]. One of the possible procedures is via the average force calculated along the path [276–278]. As mentioned above, there are difficulties in interpreting the dynamics along such a path, and one prefers to perform such computations along a true simulation trajectory, integrating over the (local) slaved coordinates and again using umbrella sampling.

Dealing with the so-called rare event problem during molecular dynamics simulations is an issue of major concern since the transition itself is often quite fast while the waiting time between successful transitions can be much longer than the available simulation time [279–285]. Recently, using Jarzynski’s inequality [286, 287] has become quite popular [288], which allows one to take rare events into account. Again, one has to be concerned whether the trajectory chosen is a reasonable reaction coordinate and whether one can treat the reaction coordinate as a slow coordinate compared to the remaining ones, which allows at least a local integration about these coordinates. Finally, grand canonical [289], semi-grand canonical [290, 291] and extended Gibbs ensemble [292] computations where atoms are essentially moved between two copies of the system [293], one describing phase A and the other phase B, (in equilibrium) have become quite popular for computing phase equilibria and differences in free energies.

As mentioned above, computing the free energies of complex phases such as alloys or solid solution phases requires more problem-specific methodologies. Such methods have their origin in simple ideal and regular solution

---

[18] A further discussion regarding various concepts of free energies is given in [267].

[19] Of course, if only the free energy difference between two phases in the same chemical system is required, then the calculational procedures can also be applied without explicit knowledge of the free energy of system B.

models and have been continuously refined [31, 294–298]. Nowadays, the cluster expansion [296, 298–301] and cluster variation [302–304] methods are among the most popular approaches, together with the explicit computation of the free energy via summing over the local free energies of a large number of atom configurations that are supposed to constitute a representative sample of the set of alloy configurations [305]. A precondition of this approach is that the basic structure (reference lattice) of the alloy is essentially independent of the distribution of the atoms over the structure or sublattices thereof (except possibly for small relaxations away from the reference positions). Then one can map the $3N$-dimensional vector $\vec{X}$ describing a given atom configuration one-to-one to an occupation state of the reference lattice [31], analogous to an n-state (Potts)-spin for n different atom types. Next one approximates the energy of the configuration by a sum over one-body, two-body, three-body, etc. interaction terms of the Potts-spins. If each atom effectively only interacts with atoms within a small neighborhood, the approximate energy function requires only a small number of interaction parameters, which can be computed via fitting the approximate energies of a set of atom configurations to the corresponding ab initio energies. Since the approximate energy function can be evaluated very quickly even for large numbers of atoms/cell, one can now calculate free energies via statistical averages over many thousands or millions of configurations to reasonably high accuracy within relatively short times [306, 307], possibly using symmetry adapted selection schemes [305] to reduce the number of energy evaluations.

4. Examples

The number of publications where at least some kind of ab initio quantum mechanical calculations are employed in the determination of phase diagrams has been rising dramatically over the past two decades, and no overview short of a dedicated monograph would be able to do them justice [36, 308].[20] These studies can be roughly separated into four different categories: prediction of a phase diagram with no input except the identity of the participating atoms [309–313], prediction of phase diagrams where all atoms have to be located on the sites of a defined set of sublattices usually known from experiment [48, 306, 314–320], validation of phase diagrams where the phases and their structures are known but all free energies of the different phases are computed without reference to additional experimental measurements [48, 240, 321–329], and finally work where experimental data are refined, typically for some important region of the phase diagram [303, 330–336]. Of course, the transition between the latter three areas of research is a gradual one. In addition, there are many investigations that focus on the prediction or determination of stable and metastable crystalline modifications in extended solids [52, 69, 337–348], molecular crystals [349–355], liquid crystals [356, 357], quasi-crystals [358], zeolites and zeolite-analogues [77, 156, 359–364], for a fixed composition, and sometimes as a function of pressure and/or temperature [365–368]. While these efforts often could be the first step in the prediction of a phase diagram, in particular if pressure and temperature are varied systematically, and many of the techniques employed can be of use in the prediction of phase diagrams, we refer the reader to a number of comprehensive reviews in the literature for an overview over these investigations [23, 55, 363, 369, 370]. Similarly, we cannot address the issue of structure prediction and phase diagrams in the context of polymers [371–373], jammed matter [374], clusters [59, 154, 155, 375, 376] and proteins [377–379]; again, a large number of reviews is available in the literature.

4.1. Prediction without any reference to experimental information

The most time-consuming step in the prediction of a phase diagram without recourse to experimental data is the exploration of the energy landscape. Although this can by now be done on an ab initio quantum mechanical level for a single composition in simple systems, in particular clusters [155, 380, 381] and periodic systems with few atoms/cell [382–384], the many optimization and exploration runs needed for complicated multinary compounds suggest the use of a modular approach [23]: In the first step, the energy landscape is explored using a robust empirical potential such as a Coulomb-plus-Lennard-Jones potential [338, 339, 385] or a Buckingham potential [386], or similar non-quantum mechanical energy or cost functions [337, 340, 387].[21] In the second step, the many hundreds of structure candidates found during global optimization and long MC/MD simulations are locally optimized on a quantum mechanical level. An important structural analysis of the structure candidates must now follow, in order to decide whether we are dealing with solid solutions/alloys or ordered crystalline modifications. The crucial issue is whether so-called structure families exist among the minima observed for many different compositions which have essentially the same energy for a given composition [66, 309]. If that is the case, the union of these local minima can be treated as a large locally ergodic region, and the free energy of this alloy phase contains an entropy of mixing which favors the alloy over ordered crystalline compounds which correspond to a single minimum basin on the energy landscape. In the case of alloys, the minimum structures belonging to such a structure family can be identified by the fact that structurally they possess the same set of sublattices on which the atoms can be more or less randomly placed. In the case of solid solutions, the same overall cation–anion superstructure is present for many compositions, and the different types of cations and/or anions are randomly distributed over the cation or anion positions in the superstructure, respectively. Finally, one can compute the free energies of the various phases for elevated temperatures e. g. in the quasi-harmonic approximation.[22]

---

[20] Although we have attempted to focus on ‘prototypical’ examples, the selection must necessarily be subjective, and we apologize in advance to the authors of all those beautiful investigations that could not be included.

[21] The parameters in these potentials reflect typical atom–atom or ion–ion distances in various chemical compounds where these atoms are found, or have been fitted to ab initio calculations.

[22] The melting transition is not directly accessible via studying only the minima of the energy landscape. Here, one needs to perform simulations at high temperatures and compute the free energy difference between the solid and liquid phases [388].

This approach has been applied to about twenty different quasi-binary alkali halide systems [309–313], where the focus was on the low temperature region of the phase diagram since the solidus–liquidus region was already known experimentally. The global landscape exploration for many different compositions was performed using simulated annealing and a Coulomb-plus-Lennard-Jones potential for the energy evaluation, and the subsequent ab initio optimizations were done using both Hartree–Fock and DFT methods, in order to be able to gain some estimate of the accuracy of the predicted low-temperature part of the phase diagram. The Gibbs free energy was computed via the convex hull method [389] using a combination of the ideal entropy of mixing and a Redlich–Kister polynomial Ansatz [390] for the enthalpy of mixing, without any input from experimental data. In all cases, the calculations correctly predicted whether a solid solution or ordered crystalline modifications were thermodynamically stable, and for those systems where the miscibility gap had been measured, the computed binodal was in good quantitative agreement with the experimental data [391] (the error in the critical temperatures of the computed miscibility gaps was estimated to be about ± 100 K), as is shown in Fig. 2 for the system NaBr–LiBr [309, 392]. For those systems where crystalline modifications were predicted to be thermodynamically stable, these agreed with those already known from experiment, and several additional stable and metastable compounds could be predicted, as is shown in Fig. 3 for the system LiBr–RbBr [310]. Such global landscape explorations as a function of composition had also been performed in the 1990s for quasi-binary systems such as Ca_2Si–$CaBr_2$ [342] and MgF_2–MgO [385], where solid solutions are not expected to occur. In these two systems, a number of (meta)stable phases were predicted, with a very promising one found at the 1:1 composition of the $CaSi_2$–$CaBr_2$ system, which was computed to be thermodynamically stable on the Hartree–Fock level.

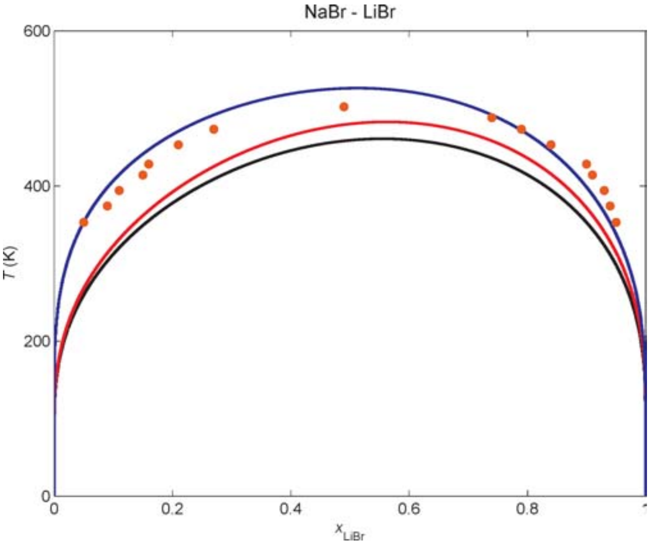

Fig. 2. Low-temperature region of the phase diagram for the system NaBr–LiBr showing the miscibility gap in the system [309]. The gap was computed using global landscape explorations followed by the determination of free enthalpies employing both Hartree–Fock (black curve) and DFT–B3LYP (red curve) calculations. The blue curve is a fit to experimental data [391]; the yellow dots are experimental data points [392].

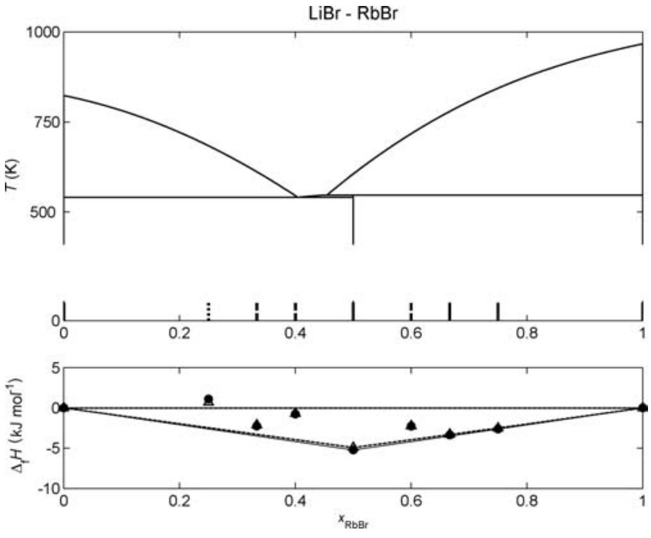

Fig. 3. Top: The phase diagram of the RbBr–LiBr system [310] computed via global landscape explorations followed by ab initio energy minimizations. Thin solid line – experimentally known high-temperature part of the phase diagram, bold solid line – predicted stable phases, dashed line – predicted metastable phases which are stable with respect to the binary compounds CsCl and LiCl, dotted line – predicted phases that are metastable with respect to the binary compounds. Bottom: Enthalpies of formation at 0 K with respect to the binary compounds for the crystalline modifications with the lowest energy for each concentration investigated. Bullets: Hartree–Fock-calculations; triangles: DFT-B3LYP-calculations.

4.2. Prediction of phase diagrams restricted to prescribed sublattices

When one tracks the development of free energy calculations of alloys, there appears a continuous path [31] from the mean-field ideal and regular solution models to the sublattice models and cluster expansion models. One goal of these latter models is to take the energy differences between the individual minima that contribute to the alloy phase into account when evaluating the free energy of mixing. Clearly, if one of these minima has a much lower enthalpy than the remaining ones, it serves as a candidate for an ordered crystalline phase, a line compound.[23] Taking this as a starting point, a number of studies have tried to predict or compute phase diagrams including both line compounds and alloy phases, on a restricted energy landscape where all atoms have to be located on the sites of a pre-defined lattice or set of sublattices, and the moveclass consists of atoms exchanging positions, possibly followed by a local minimization after each exchange [291]. The energy is then computed either via a cluster expansion model, or on an ab initio or empirical potential level, and the search for structures is performed either by Monte Carlo simulations [291], exhaustive enumeration [306], or selection from typical atom arrangements found in databases [48].

Examples of the first kind can be found in work by Allan, Barrera and co-workers [291, 393–395], who have performed semi-grand canonical simulations using ionic in-

---

[23] This is essentially the inverse approach to the general one described in the previous subsection, where each minimum is first considered as a possible line compound, and only afterwards the existence of a structure family with approximately equal minimum energies points to the existence of an alloy-like phase.

teratomic model potentials to compute phase diagrams of MgO – CaO, MgO – MnO and (Ca, Mg)CO_3 [291], all being systems that exhibit solid solution phases. No ordered phases were observed, and the agreement with experiment was again within about 100 K for the miscibility gap. In a subsequent study, the computation of the solidus – liquidus curve in the CaO – MgO system already studied earlier [396] was included [393], with good qualitative agreement with the experimental phase diagram and an underestimate of the temperature of the eutectic point of about 250 K. Results of similar quality were found in a study of the Pd – Rh system using embedded atom potentials [394] and cluster expansion methods [397].

Ceder and co-workers investigated the temperature–concentration (T, x) phase diagrams of Li_xCoO_2 [398] and Na_xCoO_2 [399], where the energy calculations were performed using effective cluster interaction terms and DFT-calculations. MC-simulations were used to explore the possible alkali metal positions on the appropriate sublattice in the alkali metal cobalt oxide structure. For certain compositions, ordered crystalline phases were observed, and furthermore several phase transitions as a function of temperature and concentration were predicted and their relation to experimental observations carefully discussed. Overall, the computed phase diagrams were in good agreement with experiment. A new phase '$NiAl_2$' stabilized by vacancies was also found in studies of the effect of vacancies on the NiAl phase diagram by Fähnle and co-workers [400]. A large number of structure types and sublattices were included in the study, and the cluster expansion technique together with DFT-calculations was employed for the energy evaluation.

An exhaustive enumeration scheme of several million atom arrangements with up to 20 atoms/unit cell on a bcc-lattice was used by Zunger and co-workers to determine possible binary ground states in the Mo – Ta system [307]. For energy calculations, again DFT was employed, together with cluster expansions including multi-site interactions. MC simulations were added in order to compute the critical temperatures for each ground state composition, leading to the prediction that at high temperatures a solid solution should be present. This prediction is in agreement with experimental data, and there are further experimental observations that support the predicted existence of ordered low-temperature structures. A similar study on a bcc lattice was performed for the Cu – Au and Ni – Pt systems [306] and the Cu – Pd system [320], where new low-temperature structures for the compositions 7 : 1 and 3 : 1 were predicted.

4.3. Prediction of phase diagrams for fixed compositions

Information about phase diagrams for fixed composition as a function of temperature and/or pressure is of great importance in many fields, especially if no reliable experimental data are accessible. In particular, the high-pressure regime has been very attractive, and many one-dimensional phase diagrams predicting high-pressure phases have been constructed [49, 52, 345 – 347, 367, 401 – 405]. Here, we are going to focus on prototypical studies where a systematic exploration of the full thermodynamic space is attempted.

All of these studies involved long MC/MD simulations at elevated temperatures since the goal was to identify possible high-temperature structures that were not associated with individual local minima on the energy landscape. Duan and co-workers performed constant (zero) pressure MD-simulations for KNO_2, $CsNO_2$ and $TlNO_2$ crystals in supercells of 432 atoms [83]. Starting in a low-temperature modification, the sample was slowly heated up, and several phase transitions were observed, until at high temperatures the nitrite group was completely free to rotate and on average an NaCl- or CsCl-type structure appeared, in good agreement with experiment. Similarly, the lattice stability of molybdenum was studied by Abrikosov and co-workers using ab initio molecular dynamics simulations on the DFT-level with about 100 atoms/cell [86]. They found that at high temperatures, the fcc-phase of Mo becomes thermodynamically metastable, although this modification does not correspond to a local minimum of the energy (the low-temperature phase is the bcc-phase) and thus is unstable at zero temperature.[24] A way to accelerate the transformation between phases during such simulations is the use of metadynamics, which has been applied in the computation of the phase diagrams of benzene [406] and silicon [407] as a function of pressure.

Finally, a construction of the free energy landscape of SrO was performed by combining runs with the ergodicity search algorithm and the threshold algorithm for a global exploration of the energy landscape [188], where an empirical Coulomb-plus-Lennard-Jones potentials served as an energy function. In the second step, the free energies of the structure candidates found were computed in the quasi-harmonic approximation on the DFT-B3LYP level. Combining these free energies as a function of temperature with the energy barriers computed via the threshold algorithm resulted in the free energy landscape shown in Fig. 4. In this system, all the relevant locally ergodic regions corresponded to basins around local minima on the energy landscape, and the appearance of the melt phase was observed by checking the stability of the underlying crystalline lattice of the rocksalt-type modification (the thermodynamically stable solid modification of SrO) during very long MC-simulation for large simulation cells as a function of temperature.[25]

4.4. Validation of phase diagrams

In addition to the landscape exploration-based computations of phase diagrams of benzene [406] and silicon [407] mentioned above, one should note the computation of the high-pressure region of the phase diagram of carbon [408], where thermodynamic integration was combined with ab initio molecular dynamics on the DFT-level to derive the phase boundaries between the various solid and liquid carbon phases. This work is in some respects a continuation of earlier investigations [409] that had focused on the properties of liquid and amorphous silicon. Another interesting study [367] covering a large range of temperatures and pressures, which also includes hypothetical candidates for new modifications, has been performed for the nitrogen-rich part of the phase diagram of the three systems Hf – N,

---

[24] For $T = 0$ K, the fcc phase of Mo is estimated to become stable above ca. 7 Mbar.

[25] Since this computation had to be performed with the empirical potential the surprisingly good agreement between theory and experiment ($T_{\text{melt}}^{\text{theo}}$ 2500 K and $T_{\text{melt}}^{\text{exp}} = 2800$ K, respectively) is only fortuitous, of course.

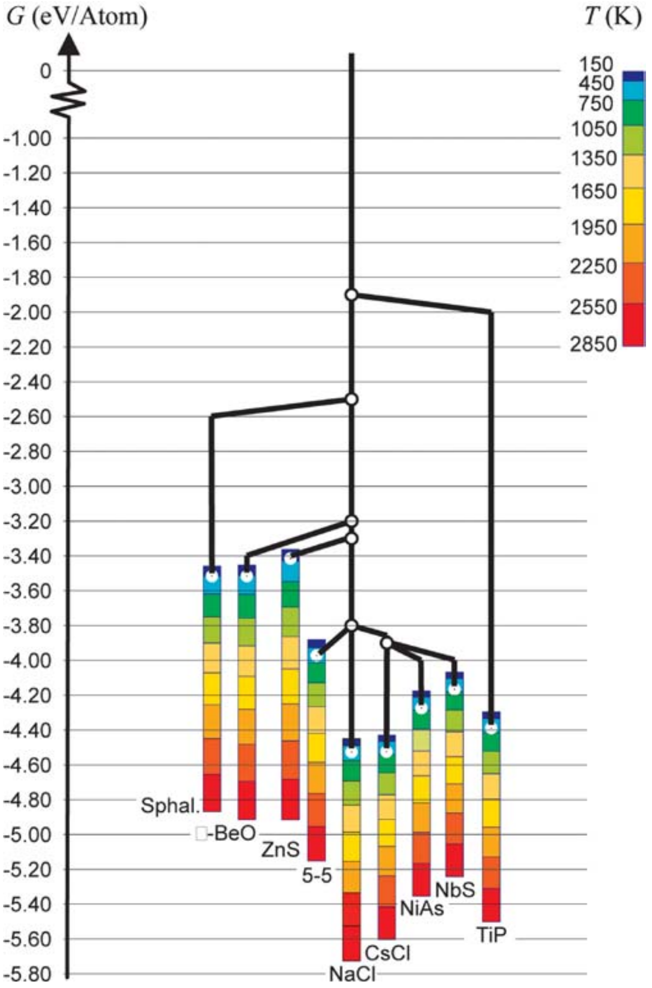

Fig. 4. Free enthalpy landscape of SrO at $p = 0$ GPa for eight different temperatures ($T = 150$ K, …, 2850 K) [188] computed using global landscape explorations followed by free energy calculations in the quasi-harmonic approximation on the empirical potential and ab initio level. The energetic contributions to the barriers stabilizing locally ergodic regions exhibiting different structure types are given by the energy difference between the minima (black circles) and transition regions (white circles). Entropic barrier contributions (for a typical example see, e. g., [186]) are not shown to avoid overloading the figure.

Zr–N, and Ti–N. The computed phase boundaries are in good qualitative agreement with the experimental results where available. Similarly good qualitative and partly quantitative agreement is found in a molecular dynamics based computation on the level of embedded atom potentials where thermodynamic integration was used to reproduce the phase diagram of the Au–Ni system [322]. Finally, a rather different type of system, noble gases and their binary mixtures, was investigated with Gibbs ensemble Monte Carlo simulations employing highly refined empirical potentials fitted to ab initio coupled-cluster calculations [323]. Very good quantitative agreement of the computed solidus–liquidus region with the experimental one was observed for most of the systems.

Clearly, central issues that need to be addressed when striving for quantitative agreement are the inclusion of vibrational degrees of freedom and the solid–liquid equilibrium. Thus, much effort has been devoted to free energy and phase diagram calculations where the vibrational entropy has been taken into consideration [240, 410–416]. Similarly, a number of studies have provided insights into the melting transition, e. g. when computing the melting point of Al [417] or melting along the shock Hugoniot of Al [418]. Other work has focused on molecular dynamics simulations of melting in ionic systems [388, 419], order–disorder phase transitions [420–422], or have tried to deduce information from simple molecular models of the solid–liquid equilibrium [423]. Finally, one should keep in mind that many structural phase transitions are associated with magnetic or electronic transitions; thus, several recent studies of iron and binary compounds containing Fe-atoms have taken magnetic contributions to the thermodynamic properties into account [242–244, 424].

5. Outlook

The prediction, determination and validation of phase diagrams employing ab initio methods have made great strides over the past two decades. At this moment, different strands of research aiming at the computation of phase diagrams with as little input from experiment as possible that had been developing essentially independently are coming together: the classical model and data-driven CALPHAD approach, the chemically inspired data mining procedures, the exhaustive generation of possible compounds and their modifications by scanning the space of periodic atom configurations or the space of possible bond-networks, and last but not least the first-principles approach described in Section 2 based on direct global exploration of the energy landscape both on the empirical potential and ab initio level.

The time thus appears ripe for pondering the next step in the field of phase diagram computations in materials science and solid state chemistry. Of course, there will be many further improvements in the accuracy of the results by performing more and more calculations with highly accurate quantum chemical methods, but as important as this kind of work is for practical applications, it constitutes only quantitative and not qualitative progress. Part of these efforts will be devoted to take subtle electronic, magnetic and elastic effects into account when computing phase diagrams, to deal with systems obeying various spatial boundary conditions (e. g. fluids or solids contained between planes or within tubes), and to predict quantum phase diagrams from first principles.

Of more fundamental importance will presumably be the determination of ‘phase diagrams’ for systems that are not close to the thermodynamic limit, for instance, finite size systems such as clusters [425, 426] or systems that have not yet reached global equilibrium. One of the major issues in this context is to what extent the traditional concept of a phase diagram that presupposes the existence of the thermodynamic limit and global equilibrium can be extended in a systematic fashion to deal with such types of systems. Possibly, it might prove necessary to introduce some new terminology to distinguish these diagrams from standard equilibrium phase diagrams. Dealing in an appropriate manner with the thermodynamics of clusters has already spawned heated discussions, e. g., regarding the issue of possible negative heat capacities in such systems [427]. In principle, such questions can be resolved within the context of locally ergodic regions and the proper observational time scales on which the movement of the cluster on the energy landscape takes place. Similarly, lack of global equilibrium leads us to acknowledge the fact that many metastable phases can co-exist on the current time scale of observation. Since this is a common situation in materials science, it appears to be worth the effort to develop some phase diagram-analogue description that allows for the existence of many metastable phases for a given set of thermodynamic conditions and/or includes the history of the experimentally determined phase diagram. Hence, the observation time scale becomes an additional parameter in the 'phase diagram', in addition to temperature, pressure, or concentration.

A natural step in this direction is the computation of so-called 'metastable phase diagrams' [428, 429]; however, it appears that for the purpose of such a computation one still starts from the assumption that all the phases are in thermodynamic equilibrium and thus employs the standard techniques, but that the thermodynamically stable phase is excluded from these calculations. Another quite interesting approach is the combination of thermodynamics and kinetic modeling visualized in the well-known time–temperature–transformation (TTT) diagrams [430–434], where the development of a phase is depicted as a function of time and temperature. These developments point in the more general direction of using tools from optimal control theory to perform phase transitions and chemical syntheses in an efficient way, both regarding the qualitative outcome (selection of a particular compound or modification as the final product) and the quantitative one (maximizing the amount of product within a given time, achieving the transition within as short a time as possible, or within a given time but with as low an entropy production or loss of availability as possible). This marriage of finite time thermodynamics [5] with phase transitions has already been achieved in the context of the gas-liquid phase transition [435], and should prove to be quite fruitful in the future. Application of such techniques to realistic systems, both with respect to the computational prediction of TTT-diagrams and the optimal control of chemical syntheses, will demand the development of efficient models of the various processes involved in a phase transition or a chemical synthesis. Examples of ongoing research whose goal is a full dynamical understanding of phase diagrams are work on spinodal decomposition [22], precipitation kinetics [436], on deriving kinetics from phase diagrams [437, 438], or work on chemical reactions [439].

However, perhaps the most fundamental change over the past two decades has been the development of a new paradigm for materials science and solid state chemistry [25, 440]: the switch from the traditional inductive approach based on explorative synthesis followed by phenomenological modeling and a posteriori interpretation and interpolation of the experimental data to a deductive one of predicting new compounds, determining the phase diagrams where they occur, and designing routes for their synthesis from first principles. This rational synthesis planning [23–25, 441] is finally coming into its own as the success of the combination of initial prediction of a new compound [347] and subsequent synthesis [442], via newly developed synthesis methods [443], clearly demonstrates [442, 444]. This transformation of solid state chemistry and materials science from an inductive to a deductive science is a monumental step, and while currently the focus is still on the development of more efficient tools to study energy surfaces and to compute phase diagrams without experimental input, perhaps an even greater challenge is faced by the experimentalist: the need for new and more refined synthesis techniques that will put into our hands the plethora of new compounds and modifications waiting for us on the energy landscapes of chemical systems.

The authors would like to acknowledge fruitful discussions at workshops on energy landscapes at the Telluride Summer Research Center in 1996, 1997, 1999, 2001, 2003, and 2005, and in Petritoli in 2007. Special thanks go to I. Pentin, D. Zagorac and M. Sultania for discussions and assistance with preparing the figures and collecting the references.

References

[1] L. Tisza: Generalized thermodynamics, MIT Press, Cambridge (USA) (1966).
[2] L. Glasser, H.D.B. Jenkins: Chem. Soc. Rev. 34 (2005) 866–874.
[3] P. Salamon, J. Nulton, J. Robinson, J.M. Pedersen, G. Ruppeiner, L. Liao: Comp. Phys. Comm. 49 (1988) 423–428.
[4] P. Salamon, P. Sibani, R. Frost: Facts, Conjectures, Improvements for Simulated Annealing, SIAM Monographs, Philadelphia (2002).
[5] S. Sieniutycz, P. Salamon: Finite Time Thermodynamics and Thermoeconomics, Taylor and Francis, New York (1990).
[6] E. Sciubba: Exergy Int. J. 1 (2001) 68–84.
[7] G. Petzow, E.T. Henig, U. Kattner, H.L. Lukas: Z. Metallkd. 75 (1984) 3.
[8] T.B. Massalski: Metall. Trans. A 20 (1989) 1295–1322.
[9] N. Saunders, A.P. Miodownik: CALPHAD (Calculation of Phase Diagrams) A comprehensive guide, Elsevier, New York (1998).
[10] R. Hockney: IEEE Trans. Comp. C 36 (1987) 231–233.
[11] J.W. Harris: Ann. Rev. Nucl. Part. Sci. 46 (1996) 71–107.
[12] S. Sachdev: Quantum phase transitions, Cambridge Univ. Press, Cambridge (2001).
[13] P. Papon, J. Leblond, P.H.E. Meijer: The physics of phase transitions, Springer, New York (2002).
[14] G.W.F. Hegel: Wissenschaft der Logik, Edition (1978) Felix-Meiner-Verlag, Hamburg (1812/13).
[15] I.E. Farquhar: Ergodic theory in statistical mechanics, Interscience, New York (1964).
[16] L.D. Landau, E.M. Lifshitz: Statistical Physics, Part 1, 3rd Ed. Pergamon, New York (1980).
[17] E.M. Lifshitz, L.P. Pitaevski: Physical Kinetics, Pergamon Press, New York (1981).
[18] J.W. Cahn, J.E. Hilliard: J. Chem. Phys. 28 (1958) 258–267.
[19] J.W. Cahn, J.E. Hilliard: J. Chem. Phys. 31 (1959) 688–699.
[20] I. Gutzow, J. Schmelzer: The Vitreous State, Springer, Berlin (1995).
[21] J.W.P. Schmelzer, G. Röpke, V.B. Priezzhev (Eds.): Nucleation Theory and Applications, JINR Dubna, Dubna (2002).
[22] J.W.P. Schmelzer, A.S. Abyzov, J. Möller: J. Chem. Phys. 121 (2004) 6900–6917.
[23] J.C. Schön, M. Jansen: Angew. Chem. Int. Ed. Eng. 35 (1996) 1286–1304.
[24] M. Jansen: Angew. Chem. Int. Ed. 41 (2002) 3747–3766.
[25] M. Jansen, in: K.M. Harris, P. Edwards (Eds.), Turning points in Solid-State, Materials and Surface Science, RSC Publishing, Cambridge, UK (2008) 22.
[26] J. Hafner: From Hamiltonians to Phase Diagrams, Springer-Verlag, Heidelberg (1987).
[27] S.R. Williams, D.J. Evans: J. Chem. Phys. 127 (2007) 184101.
[28] J.W. Gibbs: Elementary Principles in Statistical Mechanics. Developed with Special Reference to the Rational Foundations of Statistical Mechanics, Dover Publications, New York, 2nd edition (1960). Uncorrected Version of the 1st edition of Yale University Press (1902).
[29] M. Hillert: J. Alloys Comp. 320 (2001) 161–176.
[30] B. Predel, G. Oehme: Z. Metallkd. 65 (1974) 509.
[31] D. De Fontaine, in: F. Seitz, D. Turnbull, H. Ehrenreich (Eds.), Solid State Physics Vol. 47, Academic Press, New York (1994) 33–180.
[32] L. Kaufman: Calphad 1 (1977) 7–89.
[33] P. Dörner, L.J. Gauckler, H. Krieg, H.L. Lukas, G. Petzow: Calphad 3 (1979) 241.
[34] L. Kaufman, H. Nesor: Physica B 150 (1988) 99.

[35] G. Petzow, G. Effenberg: Ternary Alloys: a comprehensive compendium of evaluated constitutional data and phase diagrams, VCH, New York (1988).
[36] Z.-K. Liu, S. Hansen, J. Murray, P. Spencer, J. Saal: Comp. Coupl. Phase Diagr. Thermochem. 32 (2008) 9–31.
[37] http://www.thermocalc.com/
[38] http://www.factsage.com
[39] http://www.mtdata.software.com/
[40] http://www.computherm.com/pandat.html/
[41] R. Dovesi, C. Roetti, C. Freyria-Fava, E. Apra, V.R. Saunders, N.M. Harrison: Phil. Trans. Roy. Soc. London A 341 (1992) 203–210.
[42] W.A. Oates, H. Wenzl, T. Mohri: Calphad 20 (1996) 37–45.
[43] K. Ohno, K. Esfarjani, Y. Kawazoe: Computational Materials Science – From Ab Initio to Monte Carlo Methods, Springer, Berlin (1999).
[44] B.P. Burton, N. Dupin, S.G. Fries, G. Grimvall, A.F. Guillermet, P. Miodownik, W.A. Oates, V. Vinograd: Z. Metallkd. 92 (2001) 514–525.
[45] G.J. Ackland: J. Phys.: Cond. Matter 14 (2002) 2975–3000.
[46] C. Colinet: Intermetall. 11 (2003) 1095–1102.
[47] R. Dovesi, B. Civalleri, R. Orlando, C. Roetti, V. R. Sounders: Ab Initio Quantum Simulation in Solid State Chemistry, Vol. 21 of Reviews in Computational Chemistry, Wiley-VCH, John Wiley & Sons, Inc., Weinheim, New York (2005).
[48] S. Curtarolo, A.N. Kolmogorov, F.H. Cocks: Comp. Coupl. Phase Diagr. Thermochem. 29 (2005) 155–161.
[49] L. Stixrude, R.E. Cohen, R.J. Hemley, in: R.J. Hemley (Ed.), MSA Reviews in Mineralogy; Ultrahigh-Pressure Mineralogy, Vol. 37, Mineralogical Society of America, Washington, D.C. (1998) 639–671.
[50] B. Winkler: Z. Krist. 214 (1999) 506–527.
[51] M.L. Cohen: Phys. Stat. Sol. B 235 (2003) 221–224.
[52] Ž. Čančarević, J.C. Schön, M. Jansen: Phys. Rev. B 73 (2006) 224114.
[53] M. Goldstein: J. Chem. Phys. 51 (1969) 3728–3739.
[54] F.H. Stillinger, T.A. Weber: Phys. Rev. A 25 (1982) 978–989.
[55] J.C. Schön, M. Jansen: Z. Krist. 216 (2001) 307–325; 361–383.
[56] D.J. Wales: Energy Landscapes with Applications to Clusters, Biomolecules and Glasses, Cambridge Univ. Press, Cambridge (2003).
[57] R.S. Berry: Chem. Rev. 93 (1993) 2379–2394.
[58] D.J. Wales, J.P.K. Doye, M.A. Miller, P.N. Mortenson, T.R. Walsh, in: I. Prigogine, S.A. Rice (Eds.), Advances in Chemical Physics, Vol. 115, Wiley, New York (2000) 1–111.
[59] R. Ferrando, J. Jellinek, R.L. Johnston: Chem. Rev. 108 (2008) 845–910.
[60] L. Leuzzi, T.M. Nieuwenhuizen: Thermodynamics of the glassy state, Taylor & Francis, New York (2008).
[61] J.C. Schön, M.A.C. Wevers, M. Jansen: J. Phys.: Cond. Matter 15 (2003) 5479–5486.
[62] S.H. Northrup, J.T. Hynes: J. Chem. Phys. 73 (1980) 2700–2714.
[63] R.F. Grote, J.T. Hynes: J. Chem. Phys. 73 (1980) 2715–2732.
[64] H. Grubmüller: Phys. Rev. E 52 (1995) 2893–2906.
[65] J.-P. Aubin, A. Lesne: J. Math. Phys. 46 (2005) 043508.
[66] J.C. Schön, M. Jansen, in: J. Li, N.E. Brese, M.G. Kanatzidis, M. Jansen (Eds.), Mat. Res. Soc. Symp. Proc. Vol. 848: Solid State Chemistry of Inorganic Materials V, MRS, Warrendale (2005).
[67] A.Y. Liu, M.L. Cohen: Phys. Rev. B 41 (1990) 10727–10734.
[68] D.M. Giaquinta, H.C. zur Loye: Chem. Mater. 6 (1994) 365–372.
[69] P. Kroll, R. Hoffmann: Angew. Chem. Int. Ed. Eng. 37 (1998) 2527–2530.
[70] L. Stixrude, D.R. Peacor: Nature 420 (2002) 165–168.
[71] M.-W. Lumey, R. Dronskowski: Z. Anorg. Allg. Chem. 631 (2005) 887–893.
[72] B.P. van Eijck, W.T.M. Mooij, J. Kroon: Acta Cryst. B 51 (1995) 99–103.
[73] U. Müller, in: H. Burzlaff (Ed.), Proc. Symposium on predictability of crystal structures of inorganic solids, Friedrich-Alexander Universität Nürnberg, Nürnberg (1997) 74–88.
[74] S. Curtarolo, D. Morgan, K. Persson, J. Rodgers, G. Ceder: Phys. Rev. Lett. 91 (2003) 135503.
[75] C.C. Fischer, K.J. Tibbetts, D. Morgan, G. Ceder: Nat. Mater. 5 (2006) 641.
[76] W.E. Klee, M. Bader, G. Thimm: Z. Krist. 212 (1997) 553–558.
[77] M.M.J. Treacy, K.H. Randall, S. Rao, J.A. Perry, D.J. Chadi: Z. Krist. 212 (1997) 768–791.
[78] J. Klinowski: Curr. Opin. Solid State Mater. Sci. 3 (1998) 79–85.
[79] O. Delgado-Friedrichs, A.W.M. Dress, D.H. Huson, J. Klinowski, A.L. Mackay: Nature 400 (1999) 644–647.
[80] M.D. Foster, A. Simperler, R.G. Bell, O. Delgado-Friedrichs, F.A. Paz, J. Klinowski: Nature Mater. 3 (2004) 234–238.
[81] A. Le Bail, F. Calvayrac: J. Solid State Chem. 179 (2006) 3159–3166.
[82] O. Delgado-Friedrichs, M. O'Keefe, O.M. Yaghi: Phys. Chem. Chem. Phys. 9 (2007) 1035–1043.
[83] C.G. Duan, W.N. Mei, R.W. Smith, J. Liu, M.M. Ossowski, J.R. Hardy: Phys. Rev. B 63 (2001) 144105.
[84] R. Martonak, A. Laio, M. Parrinello: Phys. Rev. Lett. 90 (2003) 075503.
[85] D. Zahn, S. Leoni: Phys. Rev. Lett. 92 (2004) 250201.
[86] C. Asker, A.B. Belonoshko, A.S. Mikhaylushkin, I.A. Abrikosov: Phys. Rev. B 77 (2008) 220102.
[87] J.C. Schön, A. Hannemann, M. Jansen: J. Phys. Chem. B 108 (2004) 2210–2217.
[88] A. Hannemann, J.C. Schön, M. Jansen: J. Mater. Chem. 15 (2005) 1167–1178.
[89] D. Zahn: Phys. Rev. Lett. 92 (2004) 040801.
[90] I.M. Svishchev, P.G. Kusalik: Phys. Rev. Lett. 75 (1995) 3289–3292.
[91] M.H.G. Jacobs, R. Jellema, H.A.J. Oonk: Calphad 20 (1996) 79–88.
[92] A. Quandt: Lect. Notes Phys. 739 (2008) 437–469.
[93] J.C. Schön, M.A.C. Wevers, M. Jansen: J. Phys. A: Math. Gen. 34 (2001) 4041–4052.
[94] S. Wiggins: Introduction to Applied Nonlinear Dynamical Systems and Chaos, Springer, New York (1990).
[95] S. Wiggins, L. Wiesenfeld, C. Jaffé, T. Uzer: Phys. Rev. Lett. 86 (2001) 5478.
[96] K.H. Hoffmann, J.C. Schön: Found. Phys. Lett. 18 (2005) 171–182.
[97] K.H. Hoffmann, P. Sibani: Phys. Rev. A 38 (1988) 4261–4270.
[98] J.C. Gower: Biometrika 53 (1966) 325–338.
[99] C.J. Pickard, R.J. Needs: Phys. Rev. Lett. 97 (2006) 045504.
[100] B. Winkler, C.J. Pickard, V. Milman, G. Thimm: Chem. Phys. Lett. 337 (2001) 36–42.
[101] R.T. Strong, C.J. Pickard, V. Milman, G. Thimm, B. Winkler: Phys. Rev. B 70 (2004) 045101.
[102] A. Le Bail: J. Appl. Cryst. 38 (2005) 389–395.
[103] G. Ghosh, S. Delsante, G. Borzone, M. Asta, R. Ferro: Acta Mater. 54 (2006) 4977–4997.
[104] Z. Li, H.A. Scheraga: Proc. Nat. Acad. Sci. 84 (1987) 6611–6615.
[105] V. Buch, R. Martonak, M. Parrinello: J. Chem. Phys. 124 (2006) 204705.
[106] S. Kirkpatrick, C.D. Gelatt Jr., M.P. Vecchi: Science 220 (1983) 671–680.
[107] V. Czerny: J. Optim. Theo. Appl. 45 (1985) 41–51.
[108] D.J. Wales, J.P.K. Doye: J. Phys. Chem. 101 (1997) 5111–5116.
[109] M. Iwamatsu, Y. Okabe: Chem. Phys. Lett. 399 (2004) 396–400.
[110] D. Delamarre, B. Virot: RAIRO – Rech. Oper. Oper. Res. 32 (1998) 43–73.
[111] A. Möbius, A. Neklioudov, A. Diaz-Sanchez, K.H. Hoffmann, A. Fachat, M. Schreiber: Phys. Rev. Lett. 79 (1997) 4297–4301.
[112] A. Möbius, K.H. Hoffmann, J.C. Schön, in: C. Beck, G. Benedek, A. Rapisarda, C. Tsallis (Eds.), Complexity, Metastability and Nonextensivity, International School of Solid State Physics, World Scientific Singapore (2004) 215–219.
[113] G. Ruppeiner, J.M. Pedersen, P. Salamon: J. Phys. I 1 (1991) 455–470.
[114] J.A. Chandy, S. Kim, B. Ramkumar, S. Parkes, P. Banerjee: IEEE Trans. Comp. Aided Des. ICS 16 (1997) 398–410.
[115] T. Zimmermann, P. Salamon: Int. J. Comp. Math. 42 (1992) 21–32.
[116] J. Ma, D. Hsu, J.E. Straub: J. Chem. Phys. 99 (1993) 4024–4035.
[117] A. Roitberg, R. Elber: J. Chem. Phys. 95 (1991) 9277–9287.
[118] J.E. Straub, M. Karplus: J. Chem. Phys. 94 (1990) 6737–6739.
[119] J.G. Kim, Y. Fukunishi, A. Kidera, H. Nakamura: Chem. Phys. Lett. 392 (2004) 34–39.
[120] J. Pillardy, Y.A. Arnautova, C. Czaplewski, K.D. Gibson, H.A. Scheraga: Proc. Nat. Acad. Sci. 98 (2001) 12351–12356.

[121] A. Venkatnathan, G.A. Voth: J. Chem. Theo. Comp. 1 (2005) 36–40.
[122] T. Huber, W.F. van Gunsteren: J. Phys. Chem. 102 (1998) 5937–5943.
[123] B.A. Berg, H. Nogushi, Y. Okamoto: Phys. Rev. E 68 (2003) 036126.
[124] S.G. Itoh, Y. Okamoto: Chem. Phys. Lett. 400 (2004) 308–313.
[125] J. Kim, T. Keyes: J. Chem. Phys. 121 (2004) 4237–4245.
[126] B.A. Berg, T. Neuhaus: Phys. Rev. Lett. 68 (1992) 9–12.
[127] D.D. Frantz, D.L. Freeman, J.D. Doll: J. Chem. Phys. 93 (1990) 2769–2784.
[128] N. Metropolis, A.W. Rosenbluth, M.N. Rosenbluth, A.H. Teller, E. Teller: J. Chem. Phys. 21 (1953) 1087–1092.
[129] C. Tsallis: J. Stat. Phys. 52 (1988) 479–487.
[130] C. Tsallis, S.A. Stariolo: Physica A 233 (1996) 395–406.
[131] G. Dueck, T. Scheuer: J. Comp. Phys. 90 (1990) 161–175.
[132] F. Glover: Interfaces 20 (1990) 74–94.
[133] D. Cvijovic, J. Klinowski: Science 267 (1995) 664–666.
[134] M. Ji, J. Klinowski: Proc. Roy. Soc. A 462 (2006) 3613–3627.
[135] T. Huber, A. Torda, W.F. van Gunsteren: J. Comput. Aided Mol. Des. 8 (1994) 695–708.
[136] S. Goedecker: J. Chem. Phys. 120 (2004) 9911–9917.
[137] A. Laio, M. Parrinello: Proc. Nat. Acad. Sci. 99 (2002) 12562–12566.
[138] A.F. Voter: J. Chem. Phys. 106 (1997) 4665–4677.
[139] A.F. Voter: Phys. Rev. Lett. 78 (1997) 3908–3911.
[140] R.J. Wawak, J. Pillardy, A. Liwo, K.D. Gibson, H.A. Scheraga: J. Phys. Chem. A 102 (1998) 2904–2918.
[141] Y. Zhang, D. Kihara, J. Skolnick: Proteins: Struct. Funct. Gen. 48 (2002) 192–201.
[142] Z. Zhu, M.E. Tuckerman, S.O. Samuelson, G.J. Martyana: Phys. Rev. Lett. 88 (2002) 100201.
[143] H. Merlitz, W. Wenzel: Chem. Phys. Lett. 362 (2002) 271–277.
[144] D. Hamelberg, J. Morgan, J.A. McCommon: J. Chem. Phys. 120 (2004) 11919–11929.
[145] D. Hamelberg, T. Shen, J.A. McCommon: J. Chem. Phys. 122 (2005) 241103.
[146] W. Zhang, Y. Duan: Protein: Eng. Design Struct. 19 (2006) 55–65.
[147] W. Wenzel, K. Hamacher: Phys. Rev. Lett. 82 (1999) 3003–3007.
[148] K. Hamacher: Europhys. Lett. 74 (2006) 944–950.
[149] K. Hamacher: Physica A 378 (2007) 307–314.
[150] L. Cheng, W. Cai, X. Shao: Chem Phys Chem 6 (2005) 261–266.
[151] J.H. Holland: Adaptation in Natural and Artificial Systems, Univ. Mich. Press, Ann Arbor (1975).
[152] D.M. Deaven, K.M. Ho: Phys. Rev. Lett. 75 (1995) 288–291.
[153] S.M. Woodley, P.D. Battle, J.D. Gale, C.R.A. Catlow: Phys. Chem. Chem. Phys. 1 (1999) 2535–2542.
[154] R.L. Johnston, C. Roberts, in: H.M. Cartwright, L.M. Sztendera (Eds.), Soft computing approaches in chemistry, Springer-Verlag, Berlin (2003) 161–204.
[155] B. Hartke: Struct. Bonding 110 (2004) 33–53.
[156] S.M. Woodley, C.R.A. Catlow, P.D. Battle, J.D. Gale: Chem. Comm. 2004 (2004) 22–23.
[157] L.D. Lloyd, R.L. Johnston, S. Salhi: J. Comp. Chem. 26 (2005) 1069–1078.
[158] A. Diaz-Ortiz, F. Aguilera-Granja, K. Michaelian, E.O. Berlanga-Ramirez, J.M. Montejano-Carrizales, A. Vega: Physica B 370 (2005) 200–214.
[159] Y. Xiao, D.E. Williams: Chem. Phys. Lett. 215 (1993) 17–24.
[160] Y. Zeiri: Phys. Rev. E 51 (1995) R2769–R2772.
[161] V.E. Bazterra, M.B. Ferraro, J.C. Facelli: J. Chem. Phys. 116 (2002) 5984–5991.
[162] J.A. Niesse, H.R. Mayne: J. Comp. Chem. 18 (1997) 1233–1244.
[163] S. Boettcher, A.G. Percus: Phys. Rev. Lett. 86 (2001) 5211–5214.
[164] T. Klotz, S. Kobe: Acta Phys. Slov. 44 (1994) 347–356.
[165] T. Klotz, S. Schubert, K.H. Hoffmann: J. Phys.: Cond. Matt. 10 (1998) 6127–6134.
[166] P. Sibani, J.C. Schön, P. Salamon, J.-O. Andersson: Europhys. Lett. 22 (1993) 479–485.
[167] P. Sibani, P. Schriver: Phys. Rev. B 49 (1994) 6667–6671.
[168] P. Sibani, R. v. d. Pas, J.C. Schön: Comp. Phys. Comm. 116 (1999) 17–27.
[169] C. Flamm, I.L. Hofacker, P.F. Stadler, M.T. Wolfinger: Z. Phys. Chem. 216 (2002) 155–173.
[170] M.T. Wolfinger, S. Will, I.L. Hofacker, R. Backofen, P.F. Stadler: Europhys. Lett. 74 (2006) 726–732.
[171] G. Dueck: J. Comp. Phys. 104 (1993) 86–92.
[172] J.C. Schön, H. Putz, M. Jansen: J. Phys.: Cond. Matt. 8 (1996) 143–156.
[173] L. Angelani, R. Di Leonardo, G. Ruocco, A. Scala, F. Sciortino: J. Chem. Phys. 116 (2002) 10297–10306.
[174] A. Banerjee, N. Adams, J. Simmons, R. Shepard: J. Phys. Chem. 89 (1985) 52–57.
[175] R.S. Berry, H.L. Davis, T.L. Beck: Chem. Phys. Lett. 147 (1988) 13–17.
[176] I.V. Ionova, E.A. Carter: J. Chem. Phys. 98 (1993) 6377–6386.
[177] S. Fischer, M. Karplus: Chem. Phys. Lett. 194 (1992) 252–261.
[178] D.J. Wales: J. Chem. Soc. Farad. Trans. 89 (1993) 1305–1313.
[179] J.C. Mauro, R.J. Loucks, J. Balakrishnan: J. Phys. Chem. A 109 (2005) 9578–9583.
[180] G. Mills, H. Jonsson: Phys. Rev. Lett. 72 (1994) 1124–1127.
[181] H. Tanaka: J. Chem. Phys. 113 (2000) 11202–11211.
[182] E. Weinan, R. Weiqing, E. Vanden-Eijnden: Phys. Rev. B 66 (2002) 052301.
[183] G.T. Barkema, N. Mousseau: Phys. Rev. Lett. 77 (1996) 4358–4361.
[184] G. Wei, N. Mousseau, P. Derreumaux: J. Chem. Phys. 117 (2002) 11379–11387.
[185] J.C. Mauro, R.J. Loucks, J. Balakrishnan: J. Phys. Chem. B 110 (2006) 5005–5011.
[186] M.A.C. Wevers, J.C. Schön, M. Jansen: J. Phys.: Cond. Matt. 11 (1999) 6487–6499.
[187] J.D. Chodera, N. Singhal, V.S. Pande, K.A. Dill, W.C. Swope: J. Chem. Phys. 126 (2007) 155101.
[188] J.C. Schön, Ž.P. Čančarević, A. Hannemann, M. Jansen: J. Chem. Phys. 128 (2008) 194712.
[189] H.B. Schlegel: J. Comp. Chem. 24 (2003) 1514–1527.
[190] E.E. Santiso, K.E. Gubbins: Mol. Sim. 30 (2004) 699–748.
[191] E.A. Carter, C. Ciccotti, J.T. Hynes, R. Kapral: Chem. Phys. Lett. 156 (1989) 472–477.
[192] A.K. Faradijan, R. Elber: J. Chem. Phys. 120 (2004) 10880–10889.
[193] P.G. Bolhuis, C. Dellago, D. Chandler: Faraday Discuss. 110 (1998) 421–436.
[194] C. Dellago, P. Bolhuis, F.S. Csajka, D. Chandler: J. Chem. Phys. 108 (1998) 1964.
[195] C. Dellago, P. Bolhuis, P.L. Geissler, in: M. Ferrario, G. Ciccotti, K. Binder (Eds.), Computer Simulations in Condensed Matter: From Materials to Chemical Biology, Springer, New York (2006) 124.
[196] L.R. Pratt: J. Chem. Phys. 85 (1986) 5045–5048.
[197] B. Peters, W.Z. Liang, A.T. Bell, A. Chakraborty: J. Chem. Phys. 118 (2003) 9533–9541.
[198] L.Y. Chen, P.L. Nash: J. Chem. Phys. 119 (2003) 12749–12752.
[199] R.J. Dimelow, R.A. Bryce, A.J. Masters, I.H. Hillier, N.A. Burton: J. Chem. Phys. 124 (2006) 114113.
[200] H.A. Kramers: Physica VII (1940) 284–304.
[201] D.G. Truhlar, B.C. Garrett: Acc. Chem. Res. 13 (1980) 440–448.
[202] P. Hänggi, P. Talkner, M. Borkovec: Rev. Mod. Phys. 62 (1990) 251–341.
[203] E. Vanden-Eijnden, F.A. Tal: J. Chem. Phys. 123 (2005) 184103.
[204] J. Henin, C. Chipot: J. Chem. Phys. 121 (2004) 2904–2914.
[205] L. Maragliano, E. Vanden-Eijnden: Chem. Phys. Lett. 426 (2006) 168–175.
[206] B. Ensing, M. de Vivo, Z. Liu, P. Moore, M.L. Klein: Acc. Chem. Res. 39 (2006) 73–81.
[207] P. Raiteri, A. Laio, F.L. Gervasio, C. Micheletti, M. Parrinello: J. Phys. Chem. B 110 (2006) 3533–3539.
[208] J.C. Schön: Ber. Bunsenges. 100 (1996) 1388–1391.
[209] G. Hummer, I.G. Kevrekidis: J. Chem. Phys. 118 (2003) 10762–10773.
[210] J. He, Z. Zhang, Y. Shi, H. Liu: J. Chem. Phys. 119 (2003) 4005–4017.
[211] B. Alakent, M.C. Camurdan, P. Doruker: J. Chem. Phys. 123 (2005) 144910.
[212] B. Alakent, M.C. Camurdan, P. Doruker: J. Chem. Phys. 123 (2005) 144911.

[213] M.A. Amat, I.G. Kevrekidis, D. Maroudas: Phys. Rev. B 74 (2006) 132201.
[214] M.A. Amat, I.G. Kevrekidis, D. Maroudas: Appl. Phys. Lett. 90 (2007) 171910.
[215] J. Schlitter, M. Engels, P. Krüger, E. Jacoby, A. Wollmer: Mol. Sim. 10 (1993) 291–308.
[216] J. Schlitter, W. Swegat, T. Mülders: J. Mol. Model. 7 (2001) 171–177.
[217] S.A. Corcelli, J.A. Rahman, J.C. Tully: J. Chem. Phys. 118 (2003) 1085–1088.
[218] K.W. Borrelli, A. Vitalis, R. Alcantara, V. Guallar: J. Chem. Theo. Comp. 1 (2005) 1304–1311.
[219] S. Yang, J.N. Onuchic, H. Levine: J. Chem. Phys. 125 (2006) 054910.
[220] J. Hu, A. Ma, A.R. Dinner: J. Chem. Phys. 125 (2006) 114101.
[221] C. Burisch, P.R.L. Markwick, N.L. Doltsinis, J. Schlitter: J. Chem. Theo. Comp. 4 (2008) 164–172.
[222] T.V. Bogdan, D.J. Wales, F. Calvo: J. Chem. Phys. 124 (2006) 044102.
[223] J.C. Mauro, R.J. Loucks: Phys. Rev. B 76 (2007) 174202.
[224] R.H. Swendsen, A.M. Ferrenberg: Phys. Rev. Lett. 61 (1989) 2635.
[225] R.H. Swendsen, A.M. Ferrenberg: Phys. Rev. Lett. 63 (1993) 1195.
[226] F. Wang, D.P. Landau: Phys. Rev. Lett. 86 (2001) 2050.
[227] F. Wang, D.P. Landau: Phys. Rev. E 64 (2001) 056101.
[228] S. Kumar, D. Bouzida, R.H. Swendsen, P.A. Kollman, J.M. Rosenberg: J. Comp. Chem. 13 (1992) 1011.
[229] B. Roux: Comp. Phys. Comm. 91 (1995) 275–282.
[230] A.P. Lyubartsev: J. Chem. Phys. 96 (1992) 1776–1783.
[231] G.R. Smith, A.D. Bruce: Phys. Rev. E 53 (1996) 6530–6543.
[232] S.B. Opps, J. Schofield: Phys. Rev. E 63 (2001) 056701.
[233] N. Kamiya, J. Higo: J. Comp. Chem. 22 (2001) 1098–1106.
[234] F. Yasar, H. Arkin, T. Celik, B.A. Berg, H. Meirovitch: J. Comp. Chem. 23 (2002) 1127–1134.
[235] R. Jono, K. Shimizu, T. Terada: Chem. Phys. Lett. 432 (2006) 306–312.
[236] J. Kim, J.E. Straub, T. Keyes: Phys. Rev. Lett. 97 (2006) 050601.
[237] J. Kim, J.E. Straub, T. Keyes: Phys. Rev. E 76 (2007) 011913.
[238] P. Liu, G.A. Voth: J. Chem. Phys. 126 (2007) 045106.
[239] S.G. Itoh, Y. Okamoto: J. Chem. Phys. 124 (2006) 104103.
[240] G. Kern, G. Kresse, J. Hafner: Phys. Rev. B 59 (1999) 8551–8559.
[241] B. Grabowski, T. Hickel, J. Neugebauer: Phys. Rev. B 76 (2007) 024309.
[242] R. Drautz, A. Diaz-Ortiz, M. Fähnle, H. Dosch: Phys. Rev. Lett. 93 (2004) 067202.
[243] P.G. Gonzales-Ormeno, H.M. Petrilli, C.G. Schön: Scripta Mater. 54 (2006) 1271–1276.
[244] F. Körmann, A. Dick, B. Grabowski, B. Hallstedt, T. Hickel, J. Neugebauer: Phys. Rev. B 78 (2008) 033102.
[245] D. Beeman, R. Alben: Advances in Phys. 26 (1977) 339–361.
[246] O.M. Becker, M. Karplus: J. Chem. Phys. 106 (1997) 1495–1517.
[247] A. Heuer: Phys. Rev. Lett. 78 (1997) 4051–4054.
[248] D.J. Wales, M.A. Miller, T.R. Walsh: Nature 394 (1998) 758–760.
[249] S.V. Krivov, M. Karplus: J. Chem. Phys. 117 (2002) 10894–10903.
[250] T. Komatsuzaki, K. Hoshino, Y. Matsunaga, G.J. Rylance, R.L. Johnston, D.J. Wales: J. Chem. Phys. 122 (2005) 084714.
[251] A.E. Garcia, R. Blumenfeld, G. Hummer, J.A. Krumhansl: Physica D 107 (1997) 225–239.
[252] P. Garstecki, T.X. Hoang, M. Cieplak: Phys. Rev. E 60 (1999) 3219.
[253] J.P.K. Doye, C.P. Massen: J. Chem. Phys. 122 (2005) 084105.
[254] G. Cox, R.S. Berry, R.L. Johnston: J. Phys. Chem. A 110 (2006) 11543–11550.
[255] F. Noe, D. Krachtus, J.C. Smith, S. Fischer: J. Chem. Theo. Comp. 2 (2006) 840–857.
[256] F. Noe, I. Horenko, C. Schütte, J.C. Smith: J. Chem. Phys. 126 (2007) 155102.
[257] D. Gfeller, P. De Los Rios, A. Caflisch, F. Rao: Proc. Nat. Acad. Sci. 104 (2007) 1817–1822.
[258] D. Gfeller, P. De Los Rios, D. M. de Lachapelle, G. Caldarelli, F. Rao: Phys. Rev. E 76 (2007) 026113.
[259] F. Noe, S. Fischer: Curr. Opin. Struct. Biol. 18 (2008) 154–162.
[260] K.D. Ball, R.S. Berry: J. Chem. Phys. 111 (1999) 2060–2070.
[261] M.A. Miller, D.J. Wales: J. Chem. Phys. 111 (1999) 6610–6616.
[262] P. Das, M. Moll, H. Stamati, L.E. Kavraki, C. Clementi: Proc. Nat. Acad. Sci. 103 (2006) 9885–9890.
[263] A. Amadei, A.B.M. Linssen, H.J.C. Berendsen: Proteins: Struct. Funct. Gen. 17 (1993) 412–425.
[264] R. Abagyan, P. Argos: J. Mol. Biol. 225 (1992) 519–532.
[265] J.M. Troyer, F.E. Cohen: Proteins: Struct. Funct. Gen. 23 (1995) 97–110.
[266] O.M. Becker: Proteins: Struct. Funct. Gen. 27 (1997) 213–226.
[267] C. Hartmann, C. Schütte: Physica D 228 (2007) 59.
[268] J.G. Kirkwood: J. Chem. Phys. 3 (1935) 300–313.
[269] R. Zwanzig: J. Chem. Phys. 22 (1954) 1420–1426.
[270] M. Watanabe, W.P. Reinhardt: Phys. Rev. Lett. 65 (1990) 3301–3304.
[271] G.M. Torrie, J.P. Valleau: J. Comp. Phys. 23 (1977) 187–199.
[272] J.C. Schön: J. Chem. Phys. 105 (1996) 10072–10083.
[273] D.M. Zuckerman, T.B. Woolf: J. Stat. Phys. 114 (2004) 1303–1323.
[274] L. Rosso, P. Minary, Z. Zhu, M.E. Tuckerman: J. Chem. Phys. 116 (2002) 4389–4402.
[275] D.J. Wales, T.V. Bogdan: J. Phys. Chem. B 110 (2006) 20765–20776.
[276] E. Darve, A. Pohorille: J. Chem. Phys. 115 (2001) 9169–9183.
[277] X. Wu, B.R. Brooks: Chem. Phys. Lett. 381 (2003) 512–518.
[278] L. Maragliano, E. Vanden-Eijnden: J. Chem. Phys. 128 (2008) 184110.
[279] J. MacFayden, J. Wereszcynski, I. Andridioaei: J. Chem. Phys. 128 (2008) 114112.
[280] A.F. Voter: Phys. Rev. B 57 (1998) R13985–R13988.
[281] M.R. Sorensen, A.F. Voter: J. Phys. Chem. 112 (2000) 9599–9606.
[282] J. Dall, P. Sibani: Comp. Phys. Comm. 141 (2001) 260–267.
[283] R.A. Miron, K.A. Fichthorn: J. Chem. Phys. 119 (2003) 6210–6216.
[284] G. Ciccotti, M. Ferrario: J. Mol. Liquids 89 (2000) 1–18.
[285] J.A. Rahman, J.C. Tully: Chem. Phys. 285 (2002) 277–287.
[286] C. Jarzynski: Phys. Rev. Lett. 78 (1997) 2690–2693.
[287] C. Jarzynski: Phys. Rev. E 56 (1997) 5018–5035.
[288] G. Hummer, A. Szabo: Proc. Nat. Acad. Sci. 98 (2001) 3658–3661.
[289] M. Mezei: Mol. Sim. 9 (1992) 257–267.
[290] D.A. Kofke, E.D. Glandt: Mol. Phys. 64 (1988) 1105–1131.
[291] N.L. Allan, G.D. Barrera, M.Y. Lavrentiev, I.T. Todorov, J.A. Purton: J. Mater. Chem. 11 (2001) 63–68.
[292] M. Strnad, I. Nezbeda: Mol Sim. 22 (1999) 183–198.
[293] O. Delgado-Buscalioni, P.V. Coveney: J. Chem. Phys. 119 (2003) 978–990.
[294] N.S. Golosov, A.M. Tolstik: J. Phys. Chem. Solids 36 (1975) 899–902.
[295] F. Ducastelle, F. Gautier: J. Phys. F: Metal Phys. 6 (1976) 2039–2061.
[296] J.M. Sanchez, D. De Fontaine, in: Structure and Bonding in Crystals, Academic, New York (1981) 117.
[297] N. Saunders: Phil. Trans. Roy. Soc. Lond. A 351 (1995) 543–561.
[298] A.V. Ruban, I.A. Abrikosov: Rep. Prog. Phys. 71 (2008) 046501.
[299] J.W.D. Connolly, A.R. Williams: Phys. Rev. B 27 (1983) 5169–5172.
[300] D.B. Laks, L.G. Ferreira, S. Froyen, A. Zunger: Phys. Rev. B 46 (1992) 12587–12605.
[301] C. Wolverton, A. Zunger: Phys. Rev. B 50 (1994) 10548–10560.
[302] A. Gonis, X.-G. Zhang, A.J. Freeman, P. Turchi, G.M. Stocks, D.M. Nicholson: Phys. Rev. B 36 (1987) 4630–4646.
[303] P.E.A. Turchi, M. Sluiter, G.M. Stocks: J. Phase Equil. 13 (1992) 391–399.
[304] D.E. Nanu, Y. Deng, A.J. Böttger: Phys. Rev. B 74 (2006) 014113.
[305] R. Grau-Crespo, S. Hamad, C.R.A. Catlow, N.H. DeLeeuw: J. Phys.: Cond. Matter 19 (2007) 256201.
[306] M. Sanati, L.G. Wang, A. Zunger: Phys. Rev. Lett. 90 (2003) 045502.
[307] V. Blum, A. Zunger: Phys. Rev. B 69 (2004) 020103.

[308] C.M. Fang, R. Ahuja, O. Eriksson: J. Appl. Phys. 101 (2007) 013511.
[309] J.C. Schön, I.V. Pentin, M. Jansen: Phys. Chem. Chem. Phys. 8 (2006) 1778–1784.
[310] I.V. Pentin, J.C. Schön, M. Jansen: J. Chem. Phys. 126 (2007) 124508.
[311] J.C. Schön, I.V. Pentin, M. Jansen: J. Phys. Chem. B 111 (2007) 3943.
[312] J.C. Schön, I.V. Pentin, M. Jansen: Solid State Sci. 10 (2008) 455–460.
[313] I.V. Pentin, J.C. Schön, M. Jansen: Solid State Sci. 10 (2008) 804–813.
[314] M. Laradji, D.P. Landau, B. Dünweg: Phys. Rev. B 51 (1995) 4894–4902.
[315] R. Hirschl, J. Hafner, Y. Jeanvoine: J. Phys.: Cond. Matter 13 (2001) 3545–3572.
[316] C. Wolverton, V. Ozolins, M. Asta: Phys. Rev. B 69 (2004) 144109.
[317] D. Fuks, S. Dorfman, S. Piskunov, E.A. Kotomin: Phys. Rev. B 71 (2005) 014111.
[318] N.L. Allan, G.D. Barrera, M.Y. Lavrentiev, C.L. Freeman, I.T. Tordov, J.A. Purton: Comp. Mater. Sci. 36 (2006) 42–48.
[319] J.A. Purton, N.L. Allan, M. Yu. Lavrentiev, I.T. Todorov, C.L. Freeman: Chem. Geol. 225 (2006) 176–188.
[320] S. Bärthlein, G.L.W. Hart, A. Zunger, S. Müller: J. Phys.: Cond. Matter 19 (2007) 032201.
[321] G. Raabe, J. Kochler: Phys. Chem. Chem. Phys. 4 (2002) 926–930.
[322] E.O. Arregui, M. Caro, A. Caro: Phys. Rev. B 66 (2002) 054201.
[323] A.E. Nasrabad, R. Laghaei, U.K. Deiters: J. Chem. Phys. 121 (2004) 6423–6434.
[324] S. Piskunov, S. Dorfman, D. Fuks, E.A. Kotomin: Microelectr. Eng. 81 (2005) 478–484.
[325] P.G. Gonzales-Ormeno, H.M. Petrilli, C.G. Schön: Scripta Mater. 53 (2005) 751–756.
[326] S. Mehta, G.D. Price, D. Alfe: J. Phys. Chem. 125 (2006) 194507.
[327] M.Y. Lavrentiev, D. Nguyen-Manh, R. Drautz, P. Klaver, S.L. Dudarev: Phys. Chem. Chem. Phys. 5 (2003) 2190–2196.
[328] D. Nguyen-Manh, M. Yu. Lavrentiev, S.L. Dudarev: Comp. Ren. Phys. 9 (2008) 379–388.
[329] S.P. Ong, L. Wang, B. Kang, G. Ceder: Chem. Mater. 20 (2008) 1798–1807.
[330] P. Wu, G. Eriksson, A.D. Pelton, M. Blander: ISIJ Intern. 33 (1993) 26–35.
[331] G. Rubin, A. Finel: J. Phys.: Cond. Matter 7 (1995) 3139–3152.
[332] C. Wolverton, X.-Y. Yan, R. Vijayaraghavan, V. Ozolins: Acta Mater. 50 (2002) 2187–2197.
[333] J.-C. Zheng, H.-Q. Wang, A.T.S. Wee, C.H.A. Huan: Phys. Rev. B 66 (2002) 092104.
[334] Y. Wang, S. Curtarolo, C. Jiang, R. Arroyave, T. Wang, G. Ceder, L.-Q. Chen, Z.-K. Liu: Calphad 28 (2004) 79.
[335] G. Ghosh, M. Asta: Acta Mater. 53 (2005) 3225–3252.
[336] S. Shang, A.J. Böttger: Acta Mater. 53 (2005) 255–264.
[337] C.M. Freeman, J.M. Newsam, S.M. Levine, C.R.A. Catlow: J. Mater. Chem. 3 (1993) 531–535.
[338] J.C. Schön, M. Jansen: Ber. Bunsenges. 98 (1994) 1541–1544.
[339] J.C. Schön, M. Jansen: Comp. Mater. Sci. 4 (1995) 43–58.
[340] A. Takada, C.R.A. Catlow, G.D. Price: J. Phys.: Cond. Mat. 7 (1995) 8659–8692.
[341] J.C. Schön, P. Sibani: J. Phys. A: Math. Gen. 31 (1998) 8165–8178.
[342] H. Putz, J.C. Schön, M. Jansen: Z. Anorg. Allg. Chem. 625 (1999) 1624–1630.
[343] J.C. Schön, Ž. Čančarević, M. Jansen: J. Chem. Phys. 121 (2004) 2289–2304.
[344] H. Kabbour, L. Cario, F. Boucher: J. Mater. Chem. 15 (2005) 3525–3531.
[345] P. Kroll, T. Schröter, M. Peters: Angew. Chem. Int. Ed. 44 (2005) 4249–4254.
[346] Ž. Čančarević, J.C. Schön, M. Jansen: Chem. Europ. J. 13 (2007) 7330–7348.
[347] Ž. Čančarević, J.C. Schön, M. Jansen: Chem. Asian. J. 3 (2008) 561–572.
[348] V. Ozolins, E.H. Majzoub, C. Wolverton: Phys. Rev. Lett. 100 (2008) 135501.
[349] A. Gavezzotti: J. Amer. Chem. Soc. 113 (1991) 4622–4629.
[350] J.R. Holden, Z. Du, H.L. Ammon: J. Comp. Chem. 14 (1993) 422–437.
[351] R.J. Gdanitz, in: A. Gavezzotti (Ed.), Theoretical Aspects and Computer Modeling, Wiley, New York (1997) 185–201.
[352] P. Verwer, F.J.J. Leusen, in: K.B. Lipkowitz, D.B. Boyd (Eds.), Reviews of Computational Chemistry, Vol. 12, Wiley-VCH, New York, (1998) 327–365.
[353] B.P. van Eijck, J. Kroon: J. Comp. Chem. 20 (1999) 799–812.
[354] G.M. Day: Acta Cryst. B 61 (2005) 511–527.
[355] P.G. Karamertzanis, C.C. Pantelides: Mol. Phys. 105 (2007) 273–291.
[356] E.C.H. Hsu, J.F. Johnson: Mol. Cryst. Liq. Cryst. 27 (1974) 95–104.
[357] D. Chakrabarti, B. Bagchi: Proc. Nat. Acad. Sci. 103 (2006) 7217–7221.
[358] M. Mihalkovic, I. Al-Lehyani, E. Cockayne, C.L. Henley, N. Moghadam, J.A. Moriarty, Y. Wang, M. Widom: Phys. Rev. B 65 (2002) 104205.
[359] N. Engel: Acta Cryst. B 47 (1991) 849–858.
[360] C. Mellot-Draznieks, J.M. Newsam, A.M. Gorman, C.M. Freeman, G. Ferey: Angew. Chem. Int. Ed. Eng. 39 (2000) 2270–2275.
[361] C. Mellot-Draznieks, S. Girard, G. Ferey, J.C. Schön, Ž. Čančarević, M. Jansen: Chem. Eur. J. 8 (2002) 4102–4113.
[362] M.A. Zwijnenburg, S.T. Bromley, M.D. Foster, R.G. Bell, O. Delgado-Friedrichs, J.C. Jansen, T. Maschmeyer: Chem. Mater. 16 (2004) 3809–3820.
[363] C. Mellot-Draznieks: J. Mater. Chem. 17 (2007) 4348–4358.
[364] S.M. Woodley, C.R.A. Catlow: Nature Mater. 7 (2008) 937.
[365] J. Hafner: Phys. Rev. B 10 (1974) 4151–4160.
[366] H. Iyetomi, S. Ogata, S. Ichimura: Phys. Rev. B 40 (1989) 309–315.
[367] P. Kroll: J. Phys.: Cond. Matter 16 (2004) S1235–S1244.
[368] P. Carrier, R. Wentzovich, J. Tsuchiya: Phys. Rev. B 76 (2007) 064116.
[369] S.M. Woodley: Struct. Bonding 110 (2004) 95.
[370] S.L. Price: Phys. Chem. Chem. Phys. 10 (2008) 1996–2009.
[371] K.A. Dill, S. Bromberg, K. Yue, K.M. Fiebig, D.P. Yee, P.D. Thomas, H.S. Chan: Prot. Science 4 (1995) 561–602.
[372] R. Koningsveld, W.H. Stockmeyer: Polymer phase diagrams, Oxford Univ. Press, Oxford (2001).
[373] M. Muthukumar: Adv. Polym. Sci. 191 (2005) 241–274.
[374] C. Song, P. Wang, H.A. Makse: Nature 453 (2008) 629–632.
[375] N.G. Phillips, C.W.S. Conover, L.A. Bloomfield: J. Chem. Phys. 94 (1991) 4980–4987.
[376] S.K. Lai, P.J. Hsu, K.L. Wu, W.K. Liu, M. Iwamatsu: J. Chem. Phys. 117 (2002) 10715–10725.
[377] F. Rao, A. Caflisch: J. Mol. Biol. 342 (2004) 299–306.
[378] S.A. Adcock, J. A. McCammon: Chem. Rev. 106 (2006) 1589–1615.
[379] M.C. Prentiss, C. Zong, C. Hardin, M.P. Eastwood, P.G. Wolynes: J. Chem. Theo. Comp. 2 (2006) 705–716.
[380] S. Goedecker, W. Hellmann, T. Lenosky: Phys. Rev. Lett. 95 (2005) 055501.
[381] S. Yoo, X.C. Zeng: Angew. Chem. Int. Ed. 44 (2005) 1491–1494.
[382] A.R. Oganov, C.W. Glass, S. Ono: Earth Planet. Sci. Lett. 241 (2006) 95–103.
[383] K. Doll, J.C. Schön, M. Jansen: Phys. Chem. Chem. Phys. 9 (2007) 6128.
[384] K. Doll, J.C. Schön, M. Jansen: Phys. Rev. B 78 (2008) 144110.
[385] H. Putz, J.C. Schön, M. Jansen: Comp. Mater. Sci. 11 (1998) 309–322.
[386] T.S. Bush, J.D. Gale, C.R.A. Catlow, P.D. Battle: J. Mater. Chem. 4 (1994) 831–837.
[387] J. Pannetier, J. Bassas-Alsina, J. Rodriguez-Carvajal, V. Caignaert: Nature 346 (1990) 343–345.
[388] K. Harafuji, T. Tsuchiya, K. Kawamura: J. Appl. Phys. 96 (2004) 2501–2512.
[389] G.F. Voronin: Russian J. Phys. Chem. 77 (2003) 1874.
[390] O. Redlich, A.T. Kister: Ind. Eng. Chem. 40 (1948) 345.
[391] J. Sangster, A.D. Pelton: J. Phys. Chem. Ref. Data 16 (1987) 509.
[392] D. Doornhof, H.J. Van Wijk, H.A.J. Hoonk: Thermochim. Acta 76 (1984) 171.
[393] M.Y. Lavrentiev, N.L. Allan, G.D. Barrera, J.A. Purton: J. Phys. Chem. B 105 (2001) 3594–3599.

[394] F.M. Marquez, C. Cienfuegos, B.K. Pongsal, M.Y. Lavrentiev, N.L. Allan, J.A. Purton, G.D. Barrera: Model. Simul. Mater. Sci. Eng. 11 (2003) 115–126.
[395] M.Y. Lavrentiev, N.L. Allan, J.A. Purton: Phys. Chem. Chem. Phys. 5 (2003) 2190–2196.
[396] A.F. Kohan, G. Ceder: Phys. Rev. B 54 (1996) 805–811.
[397] N.A. Zarkevich, T.L. Tan, D. D. Johnson: Phys. Rev. B 75 (2007) 104203.
[398] A. Van der Ven, M.K. Aydinol, G. Ceder, G. Kresse, J. Hafner: Phys. Rev. B 58 (1998) 2975–2987.
[399] Y. Hinuma, Y.S. Meng, G. Ceder: Phys. Rev. B 77 (2008) 224111.
[400] F. Lechermann, M. Fähnle: Phys. Rev. B 63 (2000) 012104.
[401] F.C. Marton, R.E. Cohen: Amer. Mineral. 79 (1994) 789–792.
[402] J.C. Schön, M.A.C. Wevers, M. Jansen: J. Mater. Chem. 11 (2001) 69–77.
[403] Ž. Čančarević, J.C. Schön, M. Jansen: Z. Anorg. Allg. Chem. 631 (2005) 1167–1171.
[404] R. Martonak, A. Laio, M. Bernasconi, C. Ceriani, P. Raiteri, F. Ziploi, M. Parrinello: Z. Kristallogr. 220 (2005) 489–498.
[405] Ž. Čančarević, J.C. Schön, M. Jansen: Z. Anorg. Allg. Chem. 632 (2006) 1437–1448.
[406] P. Raiteri, R. Martonak, M. Parrinello: Angew. Chem. 117 (2005) 3835–3839.
[407] J. Behler, R. Martonak, D. Donadio, M. Parrinello: Phys. Rev. Lett. 100 (2008) 185501.
[408] X. Wang, S. Scandolo, R. Car: Phys. Rev. Lett. 95 (2005) 185701.
[409] G. Galli, R.M. Martin, R. Car, M. Parrinello: Phys. Rev. B 42 (1990) 7470–7482.
[410] A. Silverman, A. Zunger, R. Kalish, J. Adler: J. Phys.: Cond. Matter 7 (1995) 1167–1180.
[411] G.D. Garbulski, G. Ceder: Phys. Rev. B 53 (1996) 8993–9001.
[412] P.J. Craievich, J.M. Sanchez: Comp. Mater. Sci. 8 (1997) 92–99.
[413] X. Wang, Z.-K. Liu, L.-Q. Chen: Acta Mater. 52 (2004) 2665–2671.
[414] V. Ozolins, B. Sadigh, M. Asta: J. Phys.: Cond. Matter 17 (2005) 2197–2210.
[415] X.-Q. Chen, W. Wolf, R. Podloucky, P. Rogl: Phys. Rev. B 71 (2005) 174101.
[416] R. Arroyave, D. Shin, Z.-K. Liu: Acta Mater. 53 (2005) 1809.
[417] J. Mei, J.W. Davenport: Phys. Rev. B 46 (1992) 21–25.
[418] J.-W. Jeong, I.-H. Lee, K.J. Chang: Phys. Rev. B 59 (1999) 329–333.
[419] A. Aguado, P.A. Madden: Phys. Rev. Lett. 94 (2005) 068501.
[420] C.R. Stanek, R.W. Grimes: J. Am. Ceram. Soc. 85 (2002) 2139–2141.
[421] A. Seko, K. Yuge, F. Oba, A. Kuwabara, I. Tanaka: Phys. Rev. B 73 (2006) 094116.
[422] A. De Virgiliis, K. Binder: Phys. Rev. B 73 (2006) 134205.
[423] P.A. Monson, D.A. Kofke: Adv. Chem. Phys. 115 (2000) 113–179.
[424] D. Nguyen-Manh, M.Y. Lavrentiev, S.L. Dudarev: Comp. Mater. Sci. (2008) in press.
[425] H.-P. Cheng, X. Li, R.L. Whetten, R.S. Berry: Phys. Rev. A 46 (1992) 791–800.
[426] Z.H. Li, A.W. Jasper, D.G. Truhlar: J. Amer. Chem. Soc. 129 (2007) 14899–14910.
[427] M. Schmidt, R. Kusche, T. Hippler, J. Donges, W. Kronmüller, B. von Issendorf, H. Haberland: Phys. Rev. Lett. 86 (2001) 1191–1194.
[428] R.F. Zhang, L.T. Kong, H.R. Gong, B.X. Liu: J. Phys.: Cond. Matter 16 (2004) 5251–5258.
[429] J.H. Li, H.B. Guo, L.T. Kong, B.X. Liu: Phys. Rev. B 71 (2005) 014107.
[430] J.S. Kirkaldy, E.A. Baganis: Met. Trans. 9 (1978) 495.
[431] K. Hasiguchi, J.S. Kirkaldy, T. Fukuzumi, V. Pavaskar: CALPHAD 8 (1984) 173.
[432] M. Enomoto, H.I. Aaronson: CALPHAD 9 (1985) 43.
[433] A.A.B. Sugden, H.K.D.B. Bhadeshia: Mat. Sci. Tch. 5 (1989) 977.
[434] L. Ge, X. Hui, E.R. Wang, G.L. Chen, R. Arroyave, Z.K. Liu: Intermet. 16 (2008) 27–33.
[435] M. Santoro, J.C. Schön, M. Jansen: Phys. Rev. E 76 (2007) 061120.
[436] E. Clouet, M. Nastar: In Complex Inorganic Solids, Springer, New York (2005) 215–239.
[437] W.C.K. Poon, R. Renth, R.M.L. Evans: J. Phys.: Cond. Matter 12 (2000) A 269–A 274.
[438] B. Alling, A.V. Ruban, A. Karimi, O.E. Peil, S.I. Simak, L. Hultman, I.A. Abrikosov: Phys. Rev. B 75 (2007) 045123.
[439] A.R. Akbarzadeh, V. Ozolins, C. Wolverton: Adv. Mater. 19 (2007) 3233–3239.
[440] M. Jansen, J.C. Schön: Angew. Chem. Int. Ed. 45 (2006) 3406–3412.
[441] M. Jansen: Abh. Rhein. Westf. Akad. Wiss. N420 (1996) 7–35.
[442] Y. Liebold-Ribeiro, D. Fischer, M. Jansen: Angew. Chem. Int. Ed. 47 (2008) 4428–4431.
[443] D. Fischer, M. Jansen: Angew. Chem. Int. Ed. 41 (2002) 1755–1756.
[444] D.C. Johnson: Nature 454 (2008) 174–175.

(Received November 19, 2008; accepted December 1, 2008)

Bibliography

DOI 10.3139/146.110010
Int. J. Mat. Res. (formerly Z. Metallkd.)
100 (2009) 2; page 135–152
© Carl Hanser Verlag GmbH & Co. KG
ISSN 1862-5282

Correspondence address

Prof. Dr. J. C. Schön
Heisenbergstr. 1, D-70569 Stuttgart, Germany
Tel.: +49 711 689 1464 1500
Fax: +49 711 689 1502
E-mail: C.Schoen@fkf.mpg.de